THE DESIGN OF AN OUT-DIFFUSION EXPERIMENT AND THE USE OF GEOCHEMICAL ANALYSES FOR THE PURPOSE OF MATRIX PORE FLUID EXTRACTION AND CHARACTERIZATION: A CASE STUDY FOR RADIOACTIVE WASTE DISPOSAL

by

Katherine Elizabeth Lambie

A thesis
presented to the University of Waterloo
in fulfillment of the
thesis requirement for the degree of
Master of Science
in
Earth Sciences

Waterloo, Ontario, Canada, 2008

I hereby declare that I am the sole author of this thesis. This is a true copy of the thesis, including any required final revisions, as accepted by my examiners.

I understand that my thesis may be made electronically available to the public.

ABSTRACT

Deep crystalline rock formations of low permeability have been identified as a possible geological medium for high-level radioactive waste disposal. In order for the safe disposal of radioactive waste, a site characterization must be performed.

A comparison of site characterization methods found out-diffusion methods to be the most viable technique for pore fluid extraction.

Crush and leach, chemical and isotopic analyses such as, Cl^-, ^{37}Cl, ^{18}O, ^{2}H and ^{87}Sr were valuable in characterizing the signature/origin of the pore fluids. Variations in the signatures of the pore fluids were observed and attributed to small differences in heterogeneity within the host rock and water to rock interactions.

Estimates of the rate of effective diffusivity (De) were evaluated experimentally and with an analytical solution. Modelled De values were much greater than those determined experimentally, suggesting that the analytical solution provides a more conservative estimate of De for assessing radionuclide migration.

ACKNOWLEDGEMENTS

I would like to take this opportunity to thank Ontario Power Generation (OPG) for donating the funding for this research program. I would also like to thank Dr. Monique Hobbs from OPG and Dr. Mel Gascoyne for all your guidance, discussions and support. Your assistance with sample collection, preparation was greatly appreciated.

There are many people that I would like to thank for helping me achieve my goals in becoming a Masters graduate. First and foremost I would like to thank my thesis supervisor Dr. Shaun Frape. Your experience, vast knowledge and continued support have made this a remarkable opportunity. You have been a tremendous support throughout this entire journey and you have given me opportunities that I never would have imagined possible. I consider you more than just a thesis supervisor I consider you a true friend.

To Dr. Ed Sudicky and Dr. Bob Gillham thank you for being a part of my thesis committee and in helping me understand diffusion modelling, it was a pleasure to have had the opportunity to learn from you both.

To my wonderful fiancé Dan, thank you for all your support throughout this journey. I cannot describe how much I admire and respect you for work ethic, patience, and never-ending encouragement.

I have completed this M.Sc. for myself, but also in honour of my parents and grandparents. You have always been a tremendous support by listening and offering sound advice. I couldn't have asked for better parents or grandparents. Thank you for motivating me, encouraging me and believing in me. I love you all.

TABLE OF CONTENTS

LIST OF TABLES

LIST OF FIGURES

CHAPTER 1. INTRODUCTION

Deep crystalline rock formations of low permeability have been identified as a possible geological medium for high-level radioactive waste disposal by several international research programs, including the Geological Survey of Finland, Posiva in Finland, SKB in Sweden and the Atomic Energy of Canada Limited (AECL) (Frape and Fritz, 1987; Nordstrom et al., 1989a and Rasilainen et al., 1996).

In order for the safe disposal of radioactive waste a site characterization must be performed to predict the effectiveness in limiting radionuclide migration. This necessitates a multidisciplinary study involving the examination of the geology, mineralogy, hydrogeology and geochemistry of the plutonic rock to further understand the processes affecting groundwaters at depth, and hence their influence on a repository system (Fritz and Frape, 1982; Frape et al., 1984; Gascoyne et al., 1987).

Previous studies by Fritz and Frape, (1982) and Frape and Fritz, (1987) found that, at depths greater than 200 m groundwaters are saline as a result of a variety of processes such as water-rock interaction. Therefore, as one example of aspects important to site characterization, research should examine the water within the connected pore space (matrix pore fluid). Understanding the chemical composition of matrix pore fluid is critical in the design and location of the repository system because, the isotopic and geochemical signature of these highly saline fluids provide a better understanding of the groundwater flow system, the chemistry in crystalline rock environments and the degree of water-rock interaction at depth (for example, the extent of water to rock interaction) (Gascyone, 2004b).

The object of this study was to i) develop a more comprehensive method for extracting, and characterizing fluid compositions from rocks of low permeability, ii) to evaluate the isotopic and geochemical signature of the pore fluid using ^{18}O, ^{2}H, ^{87}Sr and Cl, iii) to assess any variations observed in the isotopic and chemical composition of the pore fluid (between each diffusion experiment) by using other techniques such as crush and leach and thin section analyses, iv) to conduct crush and leach

experiments as a comparison method to out-diffusion techniques and, iv) to estimate and compare the rate of effective diffusivity (De) using a three-dimensional model versus the experimental De results.

This out-diffusion method is of significant benefit to research programs concerned with characterizing the hydrogeochemical regime surrounding a potential deep waste repository. Geochemical and physical parameters of a rock core such as, the geochemical and isotopic signature ($\delta^{18}O$, $\delta^{2}H$, ^{37}Cl, ^{87}Sr) and diffusivity can help determine the degree of interaction of the rock and the rates of diffusion from within the rock matrix in relation to the effective permeability (Frape and Fritz, 1982; Nordstrom et al., 1989 and Rübèl et al., 2002). The study of matrix pore fluids thereby enhances our understanding of how the rock mass has evolved (chemically) with time and can help predict future water-rock compositions in the far field environment at a potential waste disposal site.

Several methods currently available for matrix pore fluid extraction include ultracentrifugation, pore water displacement, vacuum distillation and rock crush and leach. However, some of these methods are not necessarily the most viable due to high costs, incomplete extractions, and/or the influence of none mobile fluid phases such as fluid inclusions, which may significantly alter the chemical signature of the mobile pore fluids (Moreau-Le Golvan et al., 1997). Studies conducted by Couture (1983); Tullborg, (2001) and Waber and Smellie et al. (2004), concluded that given sufficient time an out-diffusion technique may be the most reasonable method for matrix pore fluid extraction, therefore our experiment was designed to test the validity of this method by developing a protocol whereby the dissolved constituents of the pore fluid could diffuse out of the rock matrix into a cell containing double deionized water, until steady-state conditions (i.e. relatively constant concentration values) were achieved. Secondly, the method would extract enough pore fluids that various geochemical and isotopic parameters (major elements, $\delta^{18}O$, $\delta^{2}H$, ^{37}Cl, ^{87}Sr) could be measured. As well, the experiments determined the diffusivity of each section of rock core and the degree of influence that grain boundary (available matrix salts in connected porosity) and fluid inclusion salts (sealed) may have on pore fluid salinity. Finally, the rates of diffusion were modeled and compared to the

experimental results and several crush and leach experiments were performed as a comparison to those conducted by AECL, (1987), Nordstrom, (1989) and Savoy, (1998).

1.1 GEOLOGICAL SETTING

The granitic rock used in the out-diffusion experiments was extracted from two boreholes drilled specifically as part of this study from the 420 m level at the Underground Research Laboratory (URL) in Pinawa, Manitoba. The URL is located within the Lac du Bonnet Batholith.

The batholith is an Archean (~2.6 Ga), grey granite-granodiorite rock type, elongated in shape, trending east-northeast within the Superior Structural Province of the Canadian Shield (Figure 1). The batholith has a surface area of 75 by 25 km and extends to a depth of about 10 km (Martin and Chandler, 1993; Brown et al., 1990; Gascoyne, 2004b).

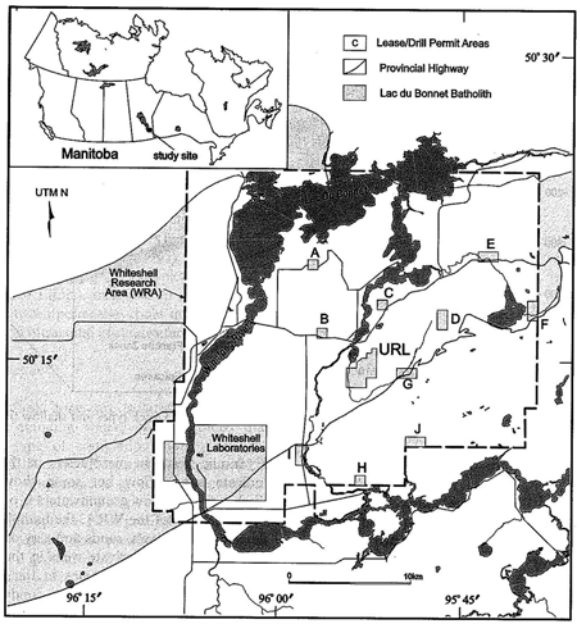

Figure 1. Site Location of the URL
The Shaded Area Represents the Lac du Bonnet Batholith (Gascoyne, 2004b)

At shallow depths (<200 m), the batholith is generally pink in colour, attributed to oxidizing conditions and contains sub vertical fractures (joints) caused by stress release following glaciations. At depths greater than 200 m, the granite is predominantly grey and sparsely fractured (Martin and Chandler 1993; Gascoyne, 2004b). The various degrees of fracturing result from the unusually high horizontal to vertical stress ratios found on site (Arjang and Herget, 1997). The URL is comprised of three main stress domains, which appear to be separated by two major thrust faults labelled fracture 2 (F2) and Fracture 3 (F3) (see Figure 2) (Haimson et al., 1993; Martin and Chandler, 1993 and Gascoyne, 2004a). Above Zone 2, the maximum principal stress is sub-horizontal, approximately 28 Mpa in magnitude, and is parallel to the major joint set. Below Fracture Zone 2 the in situ stress has rotated 90 degrees so that the maximum principal stress is aligned along the dip direction of the fracture zone. The maximum principal stress (60 Mpa) compared to the minimum principal stress (11 Mpa), produces horizontal to vertical stress ratios of about 6 to 1 (Arjang and Herget, 1997; Fairhurst, 2004; Thompson and Chandler, 2004). One of the observations reported by Haimson et al., (1993), Martin and Chandler, (1993), Arjant, and Herget, (1997), Fairhurst, (2004), Thompson and Chandler, (2004) and Gascoyne, (2004a), found that at depth (below F2) the rock was relatively unfractured because under these high stress conditions axial fractures caused by hydraulic fracturing are unable to form in sub-vertical boreholes, and in some cases the rock is unable to fracture at all As a result these high stress regimes may have an influence on the availability of matrix fluids to the fracture permeability (Frape, pers. communication).

Fracture zones are important since flow and transport along them have been found to be the predominant pathway for radionuclide migration (Fairhurst, 2004). Even sealed fractures are a concern since they may become reactivated in recent times under changing stress and neotectonic conditions and depending on stress and fluid availability may become areas of matrix fluid concentration and potential transport conduits. In addition, the various sub-horizontal fracture zones located in the uppermost 400 m control groundwater flow (Davison, 1984). These zones are further connected by sub-vertical fractures particularly in the uppermost region (~200 m) (Gascoyne et al., 1987; Gascoyne, 2004b).

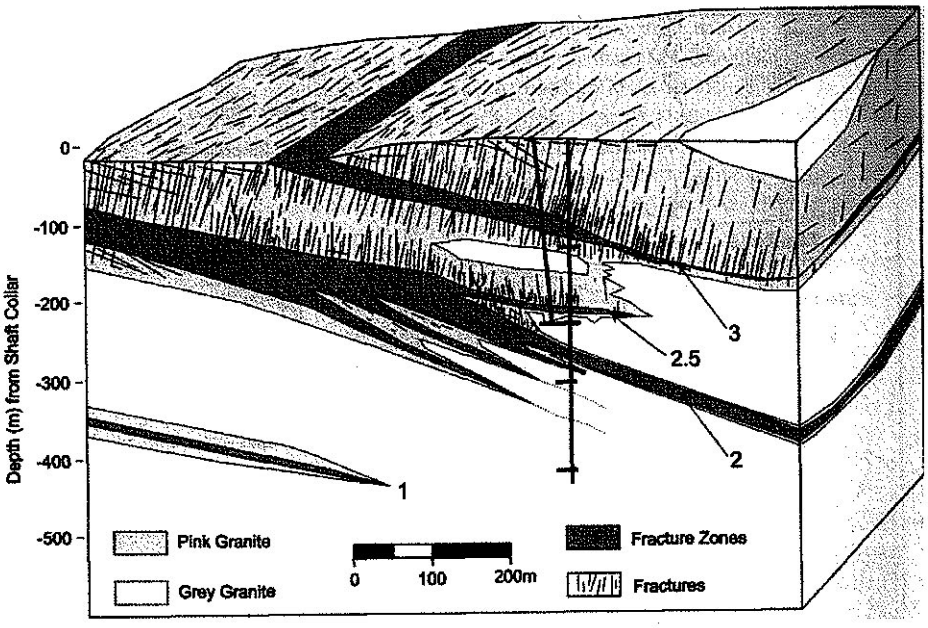

Figure 2. Cross-section of the URL
This figure indicates the Fractured Zones and Rock Types (Gascoyne, 2004a).

The hydraulic conductivity of the fracture zones within the Lac du Bonnet Batholith were found to be as high as 10^{-4} m/s. However, conductivities at depth in the unaltered, unfractured portion of the batholith range between 10^{-9} and 10^{-13} m/s. Therefore, matrix diffusion in the unaltered, unfractured crystalline rock is the limiting factor for radionuclide migration (Gascoyne, 2004a; Gascoyne, 2004b).

1.2 HYDROGEOLOGIC FLOW REGIME

Earlier studies by Stevenson et al., (1996) and Gascoyne et al., (1987) found two main flow regimes within the White Shell Research Area (WRA) near to the Lac du Bonnet study area. The area has been characterized from over 100 boreholes drilled at the site to depths of over 1000 m. These boreholes have been used to investigate the geology, hydrogeology and the geochemistry of the batholith. The two main groundwater flow systems include the shallow (<200 m) and the deep flow

regimes, each with a unique chemical composition resulting from the interaction between the water and various host rock minerals.

1.2.1 Shallow Bedrock Groundwater Chemistry

Based on studies reported by Gascoyne, (2004a), the shallow groundwater sampled from the WRA and URL has shown two geochemically distinct compositions, 1) a dilute Ca-HCO_3 water and 2) a more saline (Na-Ca-Mg-SO_4-HCO_3) type water (Gascoyne and Kamineni, 1994). The Ca-HCO_3 waters exhibit a chemical signature that is characteristic of water, which has interacted with bedrock alone. Conversely, the Na-Ca-Mg-SO_4-HCO_3 waters indicate mixing between groundwaters and overburden deposits. The dilute Ca-HCO_3 waters can be found primarily in the upland recharge zone (in the shallow bedrock or where bedrock groundwaters discharge into overburden deposits). In other bedrock samples, such as those taken near the wetland area, as groundwater migrates along the flow path it mixes with more Mg-SO_4-HCO_3 rich overburden waters and the chemical characteristic of the groundwater changes to Na- or Ca-Mg-SO_4-HCO_3 type waters, which can have TDS concentrations up to 1900 mg/L. The Mg^+ and HCO_3^- concentrations indicate that the groundwater has undergone interaction with dolomite-rich overburden deposits, and the SO_4^- is believed to have been derived from the dissolution of evaporate salts which are present in the overburden.

1.2.2 Deeper Bedrock Groundwater Chemistry

The deeper groundwaters were found to be either dilute Na-Ca-HCO_3 or contain significant amounts of Cl^- and SO_4^- (Gascoyne (2004a). With increasing depth the waters become more saline and Na-Ca-Cl-SO_4 dominated. The most saline groundwaters were found in the WRA (near the Lac du Bonnet Batholith) at a depth of 1,000 m, and TDS was found to range up to 90 g/L (Gascoyne et al., 1996). The difference in magnitude between the TDS concentration found in the overburden versus those found at depth, is attributed to increasing concentrations of Na, Ca and Cl with depth (Fritz and

Frape, 1982; McNutt et al., 1984; and Gascoyne, 2004a). In addition, due to the depletion of organic matter and CO_2 at depth, groundwaters are typically low in HCO_3 (Gascoyne, 2004a), particularly in a closed system where at depth reactions with silicate minerals can remove HCO_3 as precipitated calcite, which is a common fracture filling mineral (Gascoyne et al. 1987; Nordstrom et al., 1989a).

The deep flow regime has shown extremely high piezometric heads, which are likely the result of surface loading during the advance of the Laurentide ice sheet (Gascoyne, 2004a). Additionally, based on the hydrogeochemical data of the deep groundwaters, they are geological old and therefore are believed to have a long residence time and have a hydrogeochemical composition that is anaerobic and highly saline (Fritz and Frape, 1982). The geochemistry of the deep groundwaters (particularly the pore fluids) must be understood as groundwaters are the dominant pathway for radionuclide migration from a waste repository towards the biosphere. In addition, the chemical signature, and evolution of the groundwater (pore fluid) will provide constraints on repository design, and the modelling of the hydrogeology and the hydrogeochemistry of the system (Savoye et al., 1998).

1.2.3 Pore Fluid Composition of the Lac du Bonnet Batholith

Matrix pore fluids are defined as the accessible solution from within the rock matrix (i.e. in pockets and/or as films of fluids and salts along grain boundaries), in which its dissolved solutes have the potential to alter the fluid chemistry of the groundwater system (particularly salinity, for example) (Rasilainen et al., 1996 and Gascoyne, 2004a).

The hydrogeochemistry of the groundwater and matrix pore fluids from the Lac du Bonnet granitic batholith was determined from packer isolated borehole zones, which intersected fractures, or fault zones from within the bedrock. These boreholes were drilled from a depth of 420 m (which corresponds to the same depth as the cores used in the matrix out-diffusion experiment) to 500 m below grade. The waters were characterized using various analyses including major and minor ions, and stable and radiogenic isotopes (Gascoyne et al., 1987 and Gascoyne, 2004a).

As mentioned in Chapter 1.2.2, the deep groundwaters are alkaline, with a Na-Ca–HCO_3 composition and were found to increase in salinity with increasing distance along the flow path. The pore fluids drained from the unfractured rock at depth (420 to 500 m) were dominantly Ca-Cl in composition with a total dissolved solid (TDS) concentration of ~90 g/L (Gascoyne et al., 1996).

Gascoyne, (2004a) identified several unique chemical characteristics in the pore fluids from the Lac du Bonnet batholith. The first is the isotopic composition, which found δ^2H and $\delta^{18}O$ values to be numerically the same with a value of -15.2 ‰ (see Figure 3). As a result, the pore fluids plot to the left of the global meteoric water line (Gascoyne, 2004a). Isotopically, these values are unique as they are well displaced from other Whiteshell Research Area (WRA) groundwaters and typical Canadian Shield brines which plot closer to the Global Meteoric Water Line (GMWL) (Frape and Fritz, 1987). Given a prolonged residence time and high rock to water ratio, it is possible for the pore fluids to exhibit ^{18}O depletion over geologic time (Gascoyne, 2004a). As a result, there is still some debate regarding the possible origin and/or evolution of the pore fluids.

The second unique feature relates to the ratio of Na/Ca. The Na/Ca ratio is a commonly used parameter when evaluating the hydrogeochemical evolution of a groundwater system (Nesbitt, 1985; Nordstrom et al., 1989a). Based on studies conducted by Gascoyne, (2004a), the pore fluids from the granitic batholith were found to have a Na/Ca ratio, which decreased with increasing residence time. This is likely the result of gradual albitization of Na plagioclase. In other words, with an increase in time Na is removed to a solid phase and Ca is released into solution. Therefore, a low Na/Ca ratio suggests a long residence time (Gascoyne, 2004a).

The last unique feature to be identified in the pore fluids was the Br/Cl ratio. The presence of Br and its abundance relative to Cl helps to identify the source/origin of the fluids. The Br/Cl ratio from the pore fluids was approximately 0.0028 which lies between the range of seawater (0.0033) and basinal brines (0.001 to 0.002) suggesting that seawater may not be the sole source of these fluids (Gascoyne et al., 1987; Gascoyne, 2004a).

Although the amount of accessible pore fluid from within a crystalline rock is small, their chemical signature provides insight into the hydrogeochemical evolution of a groundwater system. They also contribute significantly to the chemistry of the groundwater system found in fracture porosity (particularly salinity) by matrix diffusion. Therefore, the study and characterization of matrix pore fluid is an important factor that must be considered when undergoing a site characterization, particularly as a possible geological medium for radioactive waste disposal (Waber and Frape, 2002).

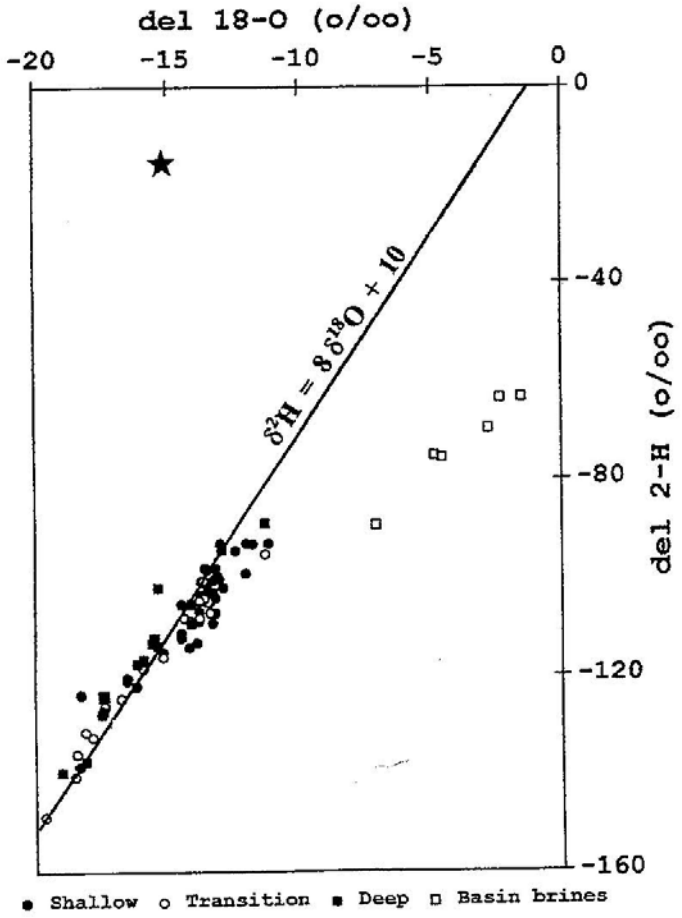

Figure 3. Diagram of ^{18}O and ^{2}H of Waters Sampled from Various Waters within the Whiteshell Research Area with Respect to the Global Meteoric Water Line (GMWL)

The star marks the isotopic composition of the pore fluids from the 420 m level of the URL (Gascoyne, 2004b).

CHAPTER 2. BACKGROUND

2.1 MATRIX DIFFUSION

As discussed in Chapter 1.2, matrix pore fluids are potential pathways for radionuclide migration. The process in which the dissolved solutes of the pore fluid are extracted from the rock matrix and enter into the groundwater system is known as matrix diffusion, and it is one of the most important pathways for pore fluid/salt migration. Therefore, matrix diffusion can be an important process controlling radionuclide migration within the subsurface (Rasilainen et al., 1996; Boving et al., 2001; Gascoyne, 2004a; Liu et al., 2004).

Several methods for extracting the matrix pore fluid solutes have been used on a variety of rock types with low hydraulic conductivity. The most common of these are, vacuum distillation, pore water displacement, equilibration during out diffusion experiments and rock core crush and leach techniques (Rübèl et al., 2002; Smellie et al., 2003 and Waber and Smellie, 2004). The results from these studies found that vacuum distillation methods were not without difficulties. For example, the sensitivity of isotope analyses is based on the yield of extraction (i.e. fractionation between extracted and non-extracted water), contact time with the atmosphere (i.e. a shift was observed in the $\delta^{18}O$ values) and the temperature at which distillation took place. The results from the pore water displacement technique established that removal of all accessible pore fluid was ultimately difficult and unattainable (Moreau-Le Glovan et al., 1997 and Rübèl et al. 2002). Crush and leach methods have also been examined as a viable means of extracting and characterizing pore fluid compositions (such as salinity). The pore fluids (i.e. the constituents of the fluid) extracted is not only from grain boundary salts but also from trapped fluid known as fluid inclusions. However, this method cannot distinguish between the origin and the potential contribution that each component may have on the overall pore fluid salinity (Savoye et al., 1998). Consequently, in order to infer in-situ pore fluid composition, this method must be used in conjunction with other methods such as matrix out diffusion (Smellie et al., 2003 and Rübèl, et al., 2002).

Previous matrix pore fluid chemistry experiments have been carried out on crystalline rock from the Äspö Hard Rock Laboratory in Sweden and Olkiluto in Finland. These studies evaluated several pore fluid extraction methods including an out-diffusion experiment on rocks with low hydraulic conductivity (and fracture frequency) (Waber, and Frape 2002; Smellie et al., 2003 and Waber and Smellie, 2004). Based on their findings, it was proposed that given sufficient time, the dissolved components within the matrix pore fluid could be successfully diffused into an enclosed water reservoir and reach steady-state conditions. Steady-state conditions are defined as a state of equilibrium between the water and the host rock, whereby the rock has released all of the constituents of the pore fluid. Therefore, in theory the concentration of the non-reactive solutes (i.e. Cl) extracted (through diffusion) from a rock core can be used to calculate the original pore fluid composition.

Based on the diffusion experiment conducted by Waber and Frape, (2002), at early time an initial pulse of highly saline pore fluid was observed. The pulse of highly saline pore fluid is most likely attributed to fluid inclusion leakage due to fractures formed from drilling of the core and initial stress release. Drilling releases lithostatic pressure, which causes the rock core to develop microfractures, particularly in the outer exposed surface of the core. This increases the potential for fluid inclusions (surrounding the fracture zones) to rupture and release a pulse of highly saline fluid into the nearby fracture zone(s) or experimental reservoir.

In addition to Waber and Frape (2002), the diffusion experiments conducted by Smellie et al., (2003), were unsuccessful in determining an in-situ pore water composition because the bulk solution within the reaction vessel/experimental reservoir had not homogenized. Therefore, concentration gradients existed between the top and bottom of the reservoir. For example, the bulk solution and the constituents of the extracted pore fluid had not undergone complete mixing therefore, the solution at the top of the water column differed from concentrations measured from samples obtained from the base of the reservoir. Nonetheless, given sufficient time, the out-diffusion experiments are anticipated to be the best method for extracting and characterizing matrix pore water compositions and diffusive rock properties.

2.2 CHLORIDE

Chloride is a major component in deep groundwater systems, such as the crystalline rock environment at the URL (Fritz and Frape, 1982; Frape and Fritz, 1987; Gascoyne et al., 1987).

Chloride is an important constituent because it is one of the most conservative ions. Therefore, Cl is frequently used as an indicator parameter for identifying chemical compositional changes within water reservoirs versus the use of more reactive ions (Eastoe et al., 1989 and Nordstrom et al., 1989). In addition, ionic chloride (Cl^-) is relatively conservative (i.e. non-reactive) in solution over a large range of temperatures and pressures, and does not readily adsorb onto clays. Furthermore, Cl does not enter readily into oxidation-reduction reactions under normal groundwater pH-Eh conditions (Kaufmann et al., 1988). As a result, Cl has been utilized in many diffusion experiments as a conservative tracer to identify diffusive loading from the rock matrix and eventually as an indicator of steady-state conditions (Nordstrom et al., 1989 and Gascoyne et al., 1989 and Smellie et al., 2003).

Chloride is also a valuable tool for identifying the origin, and evolutionary trend of a groundwater system, based on its relationship with respect to other elements such as strontium. For example, if there is a positive relationship between Cl and Sr values then it may be indicative of a single source zone, in other words, a common origin and/or evolutionary trend (McNutt et. al., 1989).

Chloride concentrations are also useful when determining the extent of water-rock interaction by comparing the loss or gain of other ions versus the conservative nature of chloride (Nordstrom et al., 1989a; Waber and Smellie, 2004; Vilks et al., 1999 Smellie et al., 2003).

2.3 CRUSH AND LEACH

Crush and leach is a viable method for extracting and characterizing pore fluid salinity, because, it releases fluid inclusions and grain boundary salts that would otherwise be unattainable if the

rock were not severely fractured or altered (Savoye et al., 1998). Fluid inclusions as defined by Nordstrom et al., (1989b) and Roedder (1984) are natural porosity filled with substances, such as NaCl (although many different compositions exist), that were trapped during the formation of a mineral. The inclusion is defined as "primary" if it formed with the growth of the mineral or "secondary" if it formed after the initial mineral formation (i.e. after a mineral had fractured and rehealed). They may exist in solid, liquid or vapour form or any combination thereof, and are ubiquitous in calcite (fracture filling mineral) and quartz (matrix mineral). Calcite (in fractures) and quartz (in the matrix) are commonly used in fluid inclusion studies because they are representative of the paleo-hydro environment (fractures) and the primary intrusive environment (matrix) of a crystalline rock (Larson and Tullborg 1983; Clauer et al. 1989, McNutt et al. 1990; Blyth 2004).

Fluid inclusions are important in deep crystalline rock environments because studies conducted by (Fritz et al., 1979; Nordstrom et al., 1989b and Savoye, 1998) found that fluid inclusion leakage can contribute significantly to the salinity of the groundwater system. As discussed in Chapter 1, recent studies conducted by Gascoyne, (2004a), found enough soluble chloride in fluid inclusions from the granitic rock of the Lac du Bonnet batholith to contribute as much as 90 g Cl/L to the groundwater composition. This represents a significant contribution of Cl to a slow-moving groundwater system (Gascoyne et al., 1989).

In order to determine the contribution of fluid inclusion leakage to pore and groundwater salinity, several crush and leach methods have been historically used (Savoye, 1998; Lindblom et al., 2002; Blyth, 2004). However, as mentioned in Chapter 2.1, the main difficulty with crush and leach is distinguishing between the Cl contribution from grain boundary salts (i.e. matrix salts) versus isolated fluid inclusions, and the contribution of salts from the breakdown of minerals (i.e. OH^- sites substituted for Cl minerals). Understanding the relative contribution of Cl from each source to the groundwater system is important when trying to assess their potential impact on the geochemical system surrounding a repository (Nordstrom et al., 1989b). In other words, should the crystalline rock environment become disturbed (i.e. fractured) the release of Cl will alter the groundwater composition.

Studies conducted by (Gascoyne, 2004a; AECL, 1987; Gascoyne et al., 1989; Savoye 1998 and Blyth, 2004), found that during crush and leach experiments the amount of leachable Cl^- was proportional to the grain size. Consequently, the finer the grain sizes the more leachable Cl^-. The reason being that, the primary isolated fluid inclusions have been broken open thereby contributing to pore water salinity. However, the amount of leachable Cl^- will reach steady-state conditions at a grain size of 75 μm (AECL, 1987). In other words, at a grain size of 75 μm all the free Cl is accessible and concentrations will remain constant even at grain sizes < 75 μm (AECL, 1987).

2.4 ISOTOPIC ANALYSES

Due to the complexity of the groundwater system within the Canadian Shield, isotopic analyses have been conducted in order to fully characterize the hydrogeologic system.

Isotope analyses are a contributing approach to site characterization particularly ^{18}O, ^{2}H, ^{37}Cl and ^{87}Sr because they have been shown to provide important information regarding water-rock interactions, the relationship between paleo- hydrogeochemistry relative to present day, the residence times of groundwater systems, and the possible sources of salinity within a groundwater system (Fritz and Frape, 1982; Frape and Fritz, 1982; Frape et al., 1984; McNutt et al., 1984; McNutt et al., 1987; Frape and Fritz, 1987; Fritz et al., 1987; Nordstrom et al., 1989a; McNutt et al., 1990; Franklyn et al. 1991 and Sie and Frape, 2001).

2.4.1 $\delta^{18}O$ and $\delta^{2}H$

Globally a linear relationship for meteoric waters exists between the isotopic composition of ^{18}O and ^{2}H. This is known as the Global Meteoric Water Line (GMWL) (Craig, 1961a). The isotopic composition of groundwater and its position relative to the GMWL helps delineate the origin and chemical processes such as rock-water interaction and evaporation that may have altered groundwater chemistry with time.

Natural process such as evaporation, isotopic exchange with rock minerals, mixing of seawater and sedimentary brines would cause an isotopic shift to the right of the GMWL. A shift to the left of the GMWL was considered rare when first observed in Shield brines, but it has since been observed in studies conducted by Fritz and Frape, (1982); Frape et al. (1984); Frape and Fritz (1987); Nordstrom et al. (1989a); Kloppemann et al. (2002) and Négrel et al. (2005) (see Figure 4). Due to their isotopically distinct nature, the origin is clearly different from those of sedimentary, hydrothermal and ore-forming brines (Fritz and Frape 1982). The shift in isotopic signature is believed to be the result of mineral hydration reactions, in low water-rock ratio environments (Fritz and Frape, 1982 and Frape et al., 2004).

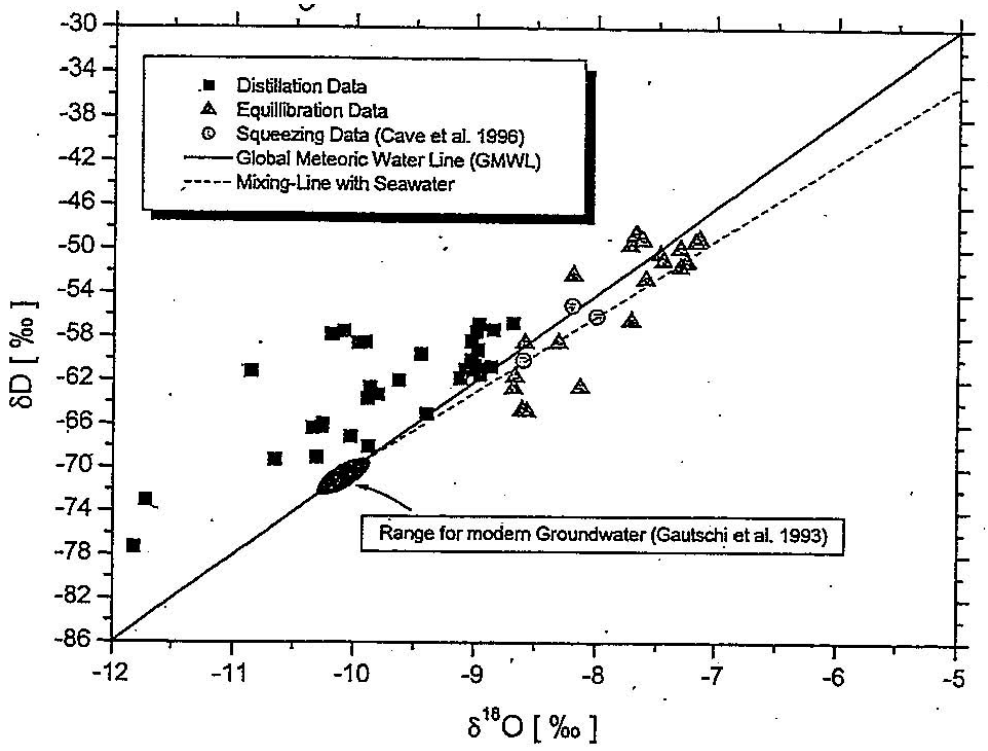

Figure 4. δ^2H and $\delta^{18}O$ from Surface and Groundwaters from the Canadian Shield

GMWL Represents the Global Meteoric Water Line ($\delta^2H=8\delta^{18}O+10‰$). Waters which plot to the right of this line (slope <8) have undergone evaporation (Rübèl et al., 2002).

Smellie et al., (2003), also found a similar enrichment in ^{18}O and ^{2}H values (relative to the GMWL) in an attempt to characterize the pore fluid (i.e. the constituents) signature of crystalline rock through the design and implementation of an out-diffusion experiment. The out-diffusion experiment was designed to allow the solutes to naturally diffuse out of the rock core into deionized water, based on concentration gradients. Further details regarding the design of the out-diffusion experiment will be discussed in Chapter 3.

Depletion in ^{18}O and enrichment in ^{2}H through water-rock interaction and low water-rock ratios was first proposed in the late 1960's, the mechanism by which this reaction occurred was most likely attributed to low-temperature isotopic exchange between minerals such as silicates and clay (Frape and Fritz 1982;, McNutt 1987 and Kloppmann et al., 2002).

Several other isotopic trends may exist including possible mixing trends between local meteoric waters and deep brines. This would generate a steep, linear slope, which would intersect the GMWL (Kloppmann et. al., 2002). Therefore, the use of isotopes (such as ^{18}O and ^{2}H) for pore fluid characterization provides insight to the hydrogeology, hydrogeochemistry water-rock interaction and the evolutionary change of groundwater at depth.

2.4.2 Chlorine Isotopes

Chlorine has two stable isotopes ^{37}Cl and ^{35}Cl with abundances of 24.23% and 75.77% respectively. As described in Chapter 2.2, chlorine does not participate readily in oxidation-reduction reactions. For this reason, researchers have observed a small range in variability for stable chlorine isotope in comparison to other stable isotopes such as hydrogen and oxygen (Eastoe et al., 1989). The largest reservoir of chloride is in seawater which has been shown to have a uniform isotopic value worldwide and therefore is assigned an isotopic signature of 0 per mil (‰), (see Chapter 3.2.4). Therefore, through isotopic investigations the fractionation of the chlorine isotopes ($^{37}Cl/^{35}Cl$) is useful because it helps to provide an understanding of the geological processes (water-rock interaction), which

alter the isotopic signature of the groundwater and the possible sources of salinity. Therefore, information regarding groundwater flow paths, mixing or evolutionary trends can be obtained and used as part of a site characterization technique for radioactive waste disposal (Hoering and Parker 1961; Eastoe et al., 1989; Sie and Frape, 2002; Frape et al., 2004; Stewart and Spivack 2004 and Shouakar-Stash et al., 2005).

Studies conducted by Sie and Frape, (2002), from the Stripa mine in Sweden, found enrichment in ^{37}Cl values with depth. Therefore, variations in ^{37}Cl can be used as an indicator for mixing between groundwaters from various depths (i.e. mixing of shallow and deep groundwater). In addition to the variation of $\delta^{37}Cl$ with depth, ^{37}Cl was found to fractionate as a result of fluid-mineral interaction. Therefore, crustal reservoirs have been found to vary significantly in Cl isotopic signature. For example, at the Stripa mine site, surface water and shallow groundwater was found to be depleted in $\delta^{37}Cl$ (i.e. reflecting present day meteoric conditions), relative to the intermediate and deep groundwaters found on site.

Chlorine isotopes can also be used when trying to assess the contribution of fluid inclusion and/or matrix salt leakage to the salinity of the groundwater system. This can be achieved by comparing the chlorine isotope signatures of the host rock and its associated fluid through progressive crush and leach experiments (crushing of the rock core to a progressively smaller grain size) such as those conducted by Savoye, (1998) and Blyth, (2004).

To date the majority of $\delta^{37}Cl$ isotopic signatures for groundwaters from crystalline rock environments have been found to lie within a narrow range, -1.0‰ to +2.0‰. However, rocks containing an abundance of Cl rich minerals such as mica, amphiboles and apatite can have Cl isotopic signatures that are quite heavy (up to 4.0‰) Therefore, a rock system can undergo a series of chemical reactions that can modify pore fluid chemistry (Frape et al., 2004).

2.4.3 Strontium ($^{87}Sr/^{86}Sr$) Ratios and Strontium Concentrations

Strontium (Sr) has four naturally occurring isotopes, ^{84}Sr, ^{86}Sr, ^{87}Sr and ^{88}Sr. All of which, with the exception of ^{87}Sr, have a relative abundance that is believed to have remained constant with time. Conversely, ^{87}Sr is a product of the radioactive decay of ^{87}Rb, which has a half-life of 4.88×10^{10} years. Therefore, as ^{87}Rb decays, ^{87}Sr increases with time and its ratio is proportional to the original concentration of Rb in each mineral (McNutt et al., (1987) and McNutt et al., (1990)).

The source of ^{87}Sr in groundwater is derived from chemical weathering and dissolution of Sr bearing mineral phases some of which contain large amounts of ^{87}Sr based on mineral and whole-rock analyses (Frape et al., 2004).

Strontium ratios have been used in many studies for evaluating the mineral phases that control water-rock interactions, groundwater chemistry and groundwater mixing. These are important processes when trying to understand and predict the evolution of groundwater chemistry with time and possible exchange reactions between a repository and the groundwater system, on both a microscopic and macroscopic scales (McNutt (2000), Frape et al., (2004), Négrel et al., (2001)).

Studies conducted by Li et al., (1989) and McNutt et al., (1990), found that a minerals $^{87}Sr/^{86}Sr$ ratio over time is dependent on the initial Rb content of the host rock, and the relative Rb/Sr ratio. This ratio (Rb/Sr) varies largely based on the dominant mineral phase present in the rock. For example, plagioclase may have a Rb/Sr content of less than 0.2 corresponding to a $^{87}Sr/^{86}Sr$ ratio between 0.70450 and 0.70679 compared to micas which, have a Rb/Sr content greater than unity, which results in a Sr ratio of greater than 0.780. Therefore, if pore fluids are believed to be in equilibrium with the host rock, then pore fluids should have the same $^{87}Sr/^{86}Sr$ ratio as the rock core. The Sr ratio has also been found to vary in groundwaters depending on their origin. Therefore, investigations of $^{87}Sr/^{86}Sr$ ratios may provide insight into the extent of water-rock interaction or suggest the possibility of mixing between two different groundwater systems (Négrel et al., (2001) and Franklyn et al., (1991)).

Based on studies conducted by (Fritz and Frape, 1982; McNutt et al., 1984; McNutt, 1987; Li et al., 1989; Franklyn et al., 1991 and Frape et al., 2004), Sr was found to have a geochemical coherence to Ca, and when Sr is plotted against Ca a positive correlation. Therefore, Sr can be used as a tracer to determine the origin of Ca, which is an important constituent in groundwaters from crystalline rock environments.

Plagioclase minerals (Ca-rich) are the dominant phase controlling Sr content in groundwater because they have been found to be the least stable mineral under low-temperature weathering conditions (Goldich (1938), McNutt (1987), Li et al., (1989), Franklyn et al., (1991) and McNutt et al., (1990). The dissolution rate of plagioclase minerals is 6.5 times faster than K-feldspar and 35 times faster than micas (muscovite) Franklyn et al., (1991). However, as the system ages, the significance of the less soluble minerals will increase, particularly in a closed system (i.e. no open fractures) with low plagioclase content. The reason being that, the solubility of plagioclase is dependent on pH, Eh, temperature and pressure. As a result, plagioclase dissolution is site dependent (Négrel et al., 2001).

2.5 DIFFUSIVITY

Diffusion models have been used in previous out-diffusion experiments in order to asses the effectiveness of laboratory derived rates of diffusion as predictive estimates of mass transport (Vilks et al., 1999 and Vilks et al., 2004). Diffusion is the process of ionic or molecular movement through a medium under a concentration gradient. When concentration gradients cease to exist (i.e. under steady-state conditions) diffusion becomes more insignificant. The diffusion process is described by Fick's first law (see equation 1) (Freeze and Cherry (1979), Boving et. al., (2001), Fetter (2001) and Liu et al., (2004)).

$$F = -\theta D \frac{\partial C}{\partial x} \tag{1}$$

F is the mass flux of solute per unit area per unit time [M/L^2T]; θ is the porosity; D is the diffusion coefficient [L^2/T] and $\partial C/\partial x$ is the concentration gradient, which is negative because the gradient vector points "up hill". The estimated diffusion coefficients for major ions (i.e. Cl^-) range between 1.0 x 10^{-9} and 2 x 10^{-9} m^2/s at 25°C (Freeze and Cherry, (1979); Boving et. al., (2001); Fetter (2001) and Liu et al., (2004)).

Diffusion can be expressed with respect to both space and time as defined by Fick's second law (equation 2). Whereby, $\partial C/\partial t$ is the change in concentration with time, and D is the diffusion coefficient of a non-adsorbed species in water. As mentioned above, D in water for Cl^- is estimated to be 1.0 x10^{-9} m^2/s (Freeze and Cherry, (1979); Vilks et al., (1999); Callahan et al., (2000); Boving et al., (2001); and Fetter, (2001)).

$$\frac{\partial C}{\partial t} = D\frac{\partial^2 C}{\partial x^2} \tag{2}$$

Diffusion in a porous medium is much slower because it is dependent upon the connected porosity and tortuosity. For example, the rate of diffusion is dependent upon the number of connected pore spaces filled with groundwater and grain size. Grain size is important because as the grains increase so does the pathway for ion migration. Therefore, in order to account for the much longer pathway (in a three-dimensional system), an effective diffusion coefficient must be considered, and is defined by D_e (Freeze and Cherry, (1979); Fetter, (2001); Rübèl et al., (2002) and Liu et al., (2004)).

$$D_e = \theta\tau D_o \tag{3}$$

Whereby, D_o is the molecular diffusion coefficient of free water (i.e. 1.0x10^{-9} m^2/s) and τ is the tortuosity factor, which cannot be measured directly, but rather using Archie's law.

$$\tau=\theta^{m-1} \tag{4}$$

Here, θ represents matrix porosity, and m is an empirical parameter that was found to be equal to 2.93 for crystalline rock environments (Liu et al., 2004).

Previous out-diffusion studies conducted by Vilks et al., (1999) and Vilks et al., (2004) found the effective diffusion coefficient for crystalline rock (from the URL) to be approximately $2.4*10^{-12}$ m^2/s, whereas the magnitude for in-situ rock diffusivity values were approximately (10^{-13} m^2/s). Studies also found significant changes in porosity and effective diffusion coefficients with depth. This suggests that the effective rate of diffusion is temperature and stress dependent; therefore as temperature increases with depth so does the rate of diffusivity. Similarly, as stress is released (upon removal of the core) the occurrence of microfracturing within the rock is also increased, thereby increasing porosity and the effective diffusivity values (Vilks et al., (1999); Boving et al., (2001) and Vilks et al., (2004)).

Total connected porosity θ is defined as,

$$\theta = V_p/V_s \tag{5}$$

Where, V_p is the volume of the pore space (L; cm^3 or m3), V_s is the total volume (unit volume of earth material, including both voids and solids L; cm^3 or m3) of the rock sample (Fetter, 2001).

Based on previous experiments conducted by Vilks et al., (1999) and Vilks et al., (2004), the most suitable method for estimating porosity (in cores with porosities less than 0.05) is the water-immersion technique. The reproducibility of porosity measurements using the water immersion technique ranges between 1 and 4%. The sensitivity of which, decreases with an increase in the mass of the core.

CHAPTER 3. METHODOLOGY

3.1 CORE PRESERVATION

As part of the present study two new boreholes, PFL1 and PFL2 were drilled at the 420 m level within the AECL's Underground Research Laboratory (URL) in Pinawa, Manitoba. Each borehole was approximately 16 m in length and 61 mm in diameter. The cores were divided and 4 segments were chosen for study. Each segment consisted of two, 15 cm sections and one, 10 cm section. The 15 cm sections were chosen for the diffusion experiment and the 10 cm sections were allocated for crush and leach experiments.

Special care was taken during the handling of the core (i.e. nitrile gloves were worn) to reduce the possibility of chloride contamination. Upon removal from the drill rod, each section was rinsed with de-ionized water before it was carefully wrapped in aluminum foil to minimize pore fluid evaporation. The sections were then labelled with the borehole number and depth, placed into plastic, cylindrical tubing, and fitted with end caps before being sealed within a plastic sleeve.

3.2 DIFFUSION EXPERIMENT

The methodology used in this experiment was a modified version of that used by Vilks et al., (1999); Rübèl, (2002); Smellie et al., (2003) and Waber and Smellie, (2004), known as an out-diffusion experiment. The out-diffusion experiments conducted by Rübèl, (2002); Smellie et al., (2003) and Waber and Smellie, (2004) involved placing a section of rock core (low permeability) into a plastic, cylindrical tube (also referred to hereafter as a "cell"). The cell was then filled with deionized water of known volume and isotopic (δ^2D and $\delta^{18}O$) signature. Given sufficient time and based on the concentration gradient within the cell (i.e. difference in concentration between the constituents/solute of

the pore fluid and the deionized water) the constituents were naturally diffused out of the rock core. As the solutes/constituents migrated out of the rock core and into the cell, the deionized water underwent a change in chemical composition, and based on the initial volume of water added to the cell, the density, porosity and volume of the rock core, the chemical composition of the pore fluid could be calculated.

The present out-diffusion experiment was based on the same principles as described above (i.e. the design of a cell and the placement of a 15 cm section of core into deionized water). However, the diffusion experiment was modified to involve the construction of two cells per experiment (one original and one duplicate) for a total of five separate out-diffusion experiments (to be conducted simultaneously). Each cell was 18 cm in height with an inside diameter of 6.9 cm. The cells were constructed from ¼" thick polycarbonate tubing, and permanently sealed at the bottom. The tops were removable, with an o-ring, and screws to provide a water and gas tight seal. The top of each cell contained two, 1/16" swagelock bulkhead sampling ports (see Figure 5).

Figure 5. Experimental Set-up for the Out-diffusion Experiment

To begin an experiment, a 15 cm section of core was un-wrapped, and the aluminium foil was set aside. The core was weighed, and placed into a diffusion cell. Approximately 300 g of water were added to ensure the core was completely submerged. In three of the experiments, ultrapure, de-oxygenated water was used, while in the remaining two experiments (cells 4 and 5), de-oxygenated, isotopically depleted water (^{2}H signature of –1000 ‰) was used (see chart below).

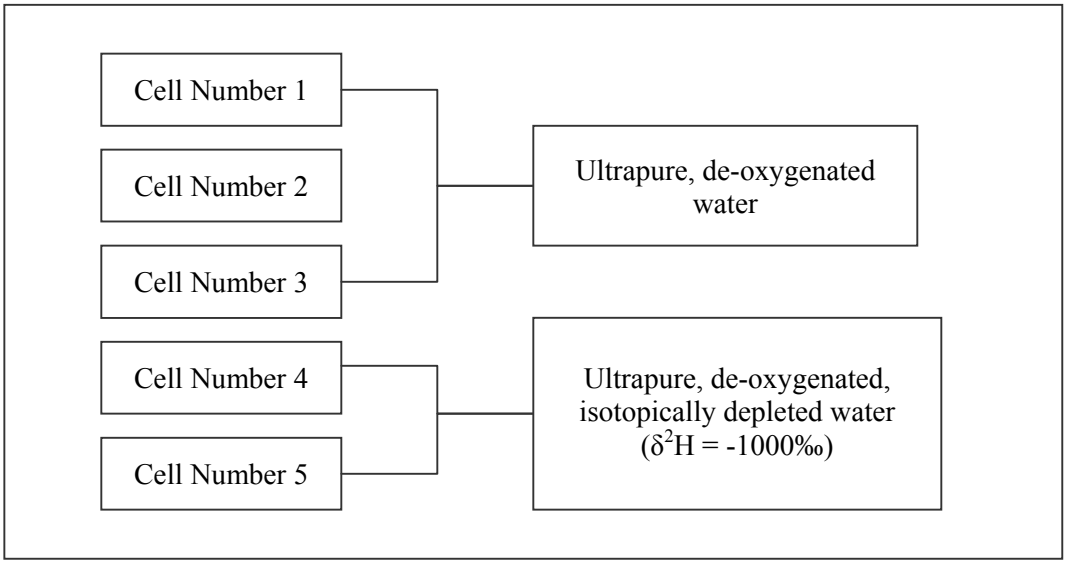

The use of such isotopically depleted water was another modification made to the original methodology as outlined by Vilks et al., (1999); Rübèl, (2002); Smellie et al., (2003) and Waber and Smellie, (2004). The purpose for using such depleted water was an attempt to show a significant shift in isotopic composition. Prior to the experiment, a blank sample of the de-oxygenated water (to be used in the experiment) was submitted to the laboratory for a dissolved oxygen (DO) and Cl measurement. This was conducted as a means of determining whether the water was in fact oxygen free, and that all measurable Cl was derived from pore fluid alone and not a background signature resulting from contamination. The laboratory results found that purging the water with ultrapure nitrogen for a

minimum of 3 hours produced a DO reading of 0.2 mg/L, suggesting concentrations well below saturation limits for oxygen. In addition, Cl analyses showed

Cl^- concentrations below the level of detection (1 ppm). The cores were then immersed into the cells, sealed and placed into a temperature controlled shaker bath set to oscillate at 20 rev/min at 45˚C. Oscillation of the cells inhibits the formation of a vertical chloride concentration gradient from forming within the cells (such as those observed in the experiment conducted by Waber and Smellie, (2004) and Smellie et al., (2003). By maintaining the system at a constant, elevated temperature the rate of diffusion was shown to increase (Waber and Smellie, 2004).

To obtain an estimate of the amount of Cl that may have leached (through diffusion or leakage of ruptured fluid inclusions) from the rock during its shipment to the laboratory, the aluminium foil that had direct contact with the core was rinsed with ultrapure water into a beaker, weighed and analyzed for chloride concentration. Any Cl, which may have been released, must be accounted for in order to back calculate the original pore fluid composition (salinity).

It should be noted that an additional diffusion experiment was conducted using an oxygen-free system. The methodology was similar to the above mentioned diffusion runs with one exception. The difference being that, ultrapure nitrogen was added to the cell during each sampling event. This inhibited oxygen from entering into the system during sampling. The experiment was allowed to run for two months in order to determine if chemical differences could be observed (i.e. significant differences in leachable Cl compared to diffusion runs 1 to 5).

One cell from each experiment was sampled with time (timed cell) to monitor the approach to steady-state, while the other remained closed (closed cell) for the duration of the experiment, and was only sampled after steady-state conditions had been achieved in the timed cells.

Sampling of the timed cells was carried out at a decreasing frequency, with the most intensive sampling in the first two weeks of the experiment. The samples were analyzed for Cl concentration, and

were plotted on a concentration versus time graph. Once the Cl concentrations appeared to be constant with increasing time, the system is thought to have reached *steady-state*. As concentration increased with time a simple diffusion model could then be used to estimate the effective diffusivity, De (Sudicky, pers. communication). Solution samples from both the timed and the closed cells were then sampled for major cations, anions, ^{18}O, ^{2}H, ^{37}Cl, ^{87}Sr, pH and alkalinity.

3.2.1 Sampling Procedure

As mentioned above, sampling was carried out at decreasing intervals in order to generate a concentration versus time graph (referred to as a breakthrough curve). This curve is necessary for modeling the rate of diffusion.

Solution samples from the timed experiments were taken using 1/16" supelco tubing and a 1 mL Luer Lok syringe (see Figure 5). The amount of water removed during each sampling event was < 0.40 g to ensure that changes in water: rock ratios were negligible. In order to produce a sufficient sample size for analysis, each 0.40 g sample was diluted using ultrapure water to a weight of 3 g. As part of the ongoing sampling/monitoring of the cells, chloride concentration was analyzed for each sampling event.

3.2.2 Major Ion, pH and Alkalinity Measurements

Once steady-state was achieved a final sampling event was conducted. This involved taking two, 75 mL samples and one 25 mL sample from each of the timed and closed cells. The 25 mL samples were used for pH and alkalinity measurements, while the 75 mL samples were analyzed for major cations and anions. The cation samples were filtered using a 0.45µm syringe filter, then acidified using concentrated, ultrapure HNO_3 until a pH<2. Anion samples were also filtered but remained unacidified. The geochemical analyses were conducted at Maxxam Analytics.

The pH and bicarbonate measurements were performed directly in the laboratory at the University of Waterloo using a portable pH meter and a Hach digital titrator. For representative pH measurements the pH buffers and the probe were equilibrated to the water temperature in the shaker bath (42°C).

3.2.3 Isotopic composition of oxygen and hydrogen

The ^{18}O and ^{2}H analyses were conducted at the University of Waterloo in the Environmental Isotope Laboratory (EIL), using a VG micromass 903 Mass Spectrometer for $^{18}0$ analyses based on a modified version of that described by Epstein and Mayeda, (1953) and continuous-flow isotope ratio mass spectrometry for ^{2}H after the methodology of Morrison et al., (2001). The results are reported using the standard δ notation and values are expressed in parts per thousand (‰), where,

$$\delta = \frac{R_{\text{sample}} - R_{\text{standard}}}{R_{\text{standard}}} \times 1000 \qquad (7)$$

and R denotes the ratio of the heavy to light isotope such as, $^{18}O/^{16}O$ or $^{2}H/^{1}H$. The standard used for calibration is defined as Vienna Standard Mean Ocean Water (VSMOW), as defined by the US National Bureau of Standards, and is provided by the International Atomic Energy Agency (IAEA). The measurable uncertainty for ^{18}O and ^{2}H is ± 0.2 ‰ and ± 1‰ respectively (Epstein and Mayeda, (1953); Craig, (1961a, b); Morrison et al., (2001) and Shouakar-Stash et al., (2007)).

3.2.4 Chlorine 37 Analysis

The methods used for stable chlorine analysis are modified after Kaufmann, (1984) and were conducted in the Environmental Isotope Laboratory (EIL) at the University of Waterloo, using a VG

micromass isoprime Mass Spectrometer. The results are also reported as the difference between the isotopic ratio of the sample and the standard, where:

$$\delta = \frac{R_{\text{sample}} - R_{\text{standard}}}{R_{\text{standard}}} \times 1000 \quad (8)$$

Units are reported as per mil (‰), and the relative standard is the $^{37}Cl/^{35}Cl$ ratio of measured seawater known as the Standard Mean Ocean Chloride, (SMOC). The consistency of the chlorine isotopic ratio in seawater permits the use of chlorine as a suitable reference standard. The analytical uncertainty for chlorine isotope measurements is within ± 0.1‰ based on repeat analyses of the samples and standards.

3.2.5 Strontium Isotopic Compositions

Strontium isotope analyses are conducted using a Triton Thermal Ionization Mass Spectrometer with a precision ranging between 0.0002 and 0.0003% (2σ), and the analyses were performed in the EIL, at the University of Waterloo. Due to the complexity of absolute Sr measurements, compared to isotopic ratio measurements all values are reported as the ratio of $^{87}Sr/^{86}Sr$.

3.2.6 Porosity Measurements

In order to calculate the original pore fluid composition (i.e. pore fluid salinity) of the rock core, the porosity of the rock core must be determined (Waber and Smellie, 2004). Therefore, several different methods for measuring porosity were conducted by AECL using core extracted from the URL. The various methods included ultracentrifugation and a modified version of the water immersion technique performed by Melynk and Skeet, (1986). The water immersion technique determines porosity based on the difference between the dry and saturated weights of the core. However, the water

immersion technique used for the present experiment was modified based on sample size, because the cores chosen for the experiment were larger than those used by Melynk and Skeet, (1986). Based on the results from each of the experiments it was concluded that due to such large sample sizes, some of the core samples might not have reached a constant dry weight under vacuum distillation after 20 days. Therefore, a second dry weight was obtained by oven drying the samples at 105 °C for one week (until a constant weight was recorded).

3.3 CRUSH AND LEACH

The crush and leach method is best used in parallel with other investigations such as mineralogical analyses (whole-rock analyses), visual analyses (such as microscope thin section analyses) and fluid inclusion analyses, in order to fully characterize the pore fluid composition and its source. The crush and leach method used was similar to that described by Waber and Smellie, (2004); Gascoyne, (2004a) and AECL, (1987) and a modified version of the progressive leaching technique performed by Savoye, (1998) and Blyth, (2004). Crush and Leach is useful because it can be performed on a variety of different grain sizes in an attempt to determine the influence of grain boundary salts and fluid inclusion leakage on pore fluid salinity (Waber and Frape, 2002 and Savoye, 1998).

Based on crush and leach experiments conducted by AECL, (1987), the water-rock ratio has a negligible impact on the amount of leachable Cl. Additionally, a leach time of greater than 20 minutes was found to provide no significant increase to the amount of Cl released (later confirmed by studies conducted at the University of Waterloo). This differs from the out-diffusion experiments, which are sensitive to water-rock ratios and leach time. However, during crush and leach, a correlation was observed between the particle size used for leaching and the amount of Cl removed. That is, Cl concentrations were shown to increase with a decrease in grain size (Waber and Frape, 2002 and Waber and Smellie, 2004).

3.3.1 Experimental Set-up

Crush and leach measurements, as a function of grain size, were conducted using one half (≈ 5 cm) of the 10 cm sections of core remaining (as described in Chapter 3.1). Gloves were worn during any handling of the core to avoid contamination. The rock sample was first placed into a plastic core bag, crushed with a rock hammer, weighed and then placed in a jaw crusher. It should be noted that the rock crusher was cleaned (with pressurized air) before and after each use in order to minimize contamination to the sample. After the rock material was removed from the jaw crusher, the total weight of material was recorded again, and then placed into a shatter box for up to 5 minutes. The shatter box further grinds the pieces into rock flour in preparation for sieving. After each use the shatter box was rinsed with de-ionized water and dried using Cl free wipes. Gloves were also worn during handling of the shatter box to prevent contamination. The weight of the rock flour was recorded, and then sieved using the following mesh sizes, 250, 180, 106, 90, 75, 63, 53 and ≤ 38 μm. Each sieved sample was individually weighed, packaged and labelled accordingly.

Sieved material of a particular grain size was placed in either a 60 mL or 120 mL clean nalgene bottle and filled with ultrapure water. In order to keep the experiment consistent and to provide sufficient sample volumes, an arbitrary water- rock ratio of 2:1 was chosen. Based on previous leaching experiments conducted by AECL, leaching times greater than 20 minutes produced a negligible difference in the amount of Cl removed. This theory was tested during the present crush and leach experiments. Therefore, the samples were set to leach (shake) for 100 minutes, with a 10 mL sample extracted every 20 minutes. The samples were extracted using a clean 10 mL syringe and filtered into a 20 mL sample vial using a 0.45 μm filter. Each individual sample (10 mL sample) was then analyzed (separately) for Cl^- concentration.

A progressive crush and leach was also conducted on core from diffusion runs #1 (timed) and diffusion run #2 (timed and closed), the purpose of which was two fold. First, to determine the influence of water-rock interaction at various grain sizes, this would then be compared to the results obtained from the diffusion experiments. Secondly, to determine the geochemical and isotopic

composition of the fluid inclusions, this would allow an assessment of the possible impact that fluid inclusion leakage has on pore water salinity. Additionally, the crush and leach method provided insight into the chemical heterogeneities observed during the present out-diffusion experiment (i.e. to explain the variation in Cl^- concentrations observed between the various diffusion runs), which will be discussed further in Chapter 4.

The progressive leaching process involved crushing the rock, recording the weight and placing the sample into a 1 L nalgene bottle. Ultrapure water was then added until a 1:1, water to rock ratio was obtained. The sample was then leached for 24 hours before sampling. Based on the timed leaching experiments mentioned above, it was concluded that 24 hours was ample time to reach steady-state concentrations under leaching conditions. Once leached, the sample was coarse filtered through a #4 filter paper, and then filtered again using a 45 μm syringe filter. The sample was then sent to the laboratory for Cl analysis. The remaining core was placed in an oven at 80°C overnight to dry and the above procedure was repeated a second and third time, but crushed to progressively finer grain size.

3.3.2 Thin Section Analyses

Eight sub-samples from diffusion experiments 1 through 5 (timed and closed) were selected for thin section analysis in an attempt to determine a correlation between the abundant mineral phases and the isotopic signatures (i.e. ^{37}Cl and ^{87}Sr) obtained through diffusion. No thin sections were constructed for borehole samples PFL 1-14 (diffusion experiment #3-timed) and PFL 2-13 (diffusion experiment #2-timed), due to insufficient sample volumes remaining after whole-rock and crush and leach analyses. The results are presented in Table A6.

The rock core from each diffusion experiment was further sub-divided and submitted to Maxxam Analytics, in Mississauga for whole-rock analysis. This procedure was conducted in order to identify major changes in mineralogical composition, which may help to explain the geochemical and isotopic differences observed between runs.

CHAPTER 4. RESULTS AND DISCUSSION

4.1 DIFFUSION EXPERIMENTS

The results of changes in chloride (Cl^-) concentration during the diffusion experiments are presented in the following chapters. The approach of the experiments to steady state was first addressed by examining the results from the five timed cells. It should be noted that the results from the oxygen-free system are also reported in the following tables.

4.1.1 Timed Cells

Five of the ten diffusion experiments were sampled exponentially for Cl^- concentrations during a six-month period. The results for all five runs and the oxygen-free experiment are plotted on Figure 6 and 7, and are tabulated in Table A1 of Appendix A.

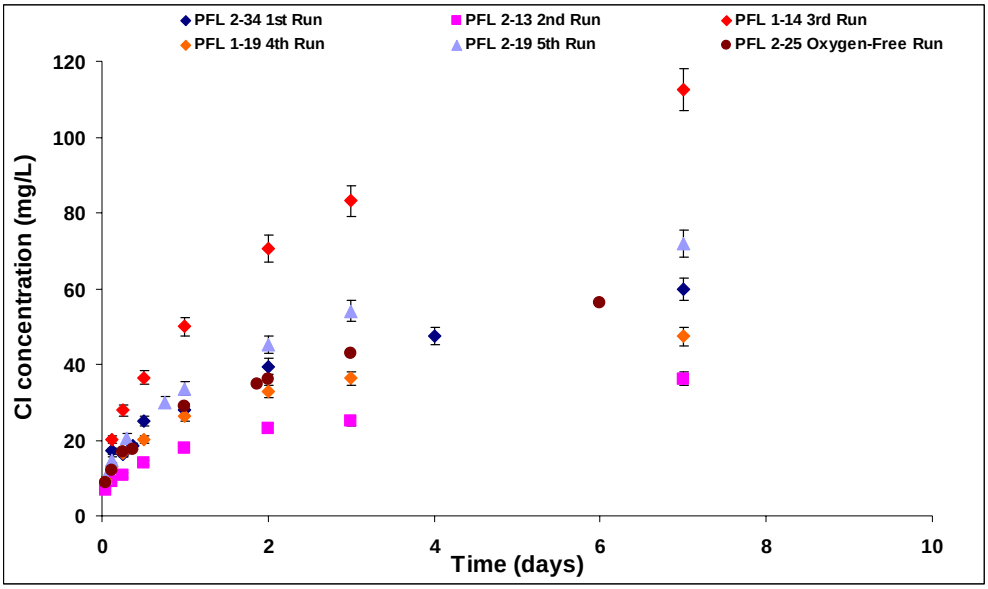

Figure 6. Detail, Showing Cl Concentration Measured in Solution at Early Times for All Five, Timed Diffusion Experiments

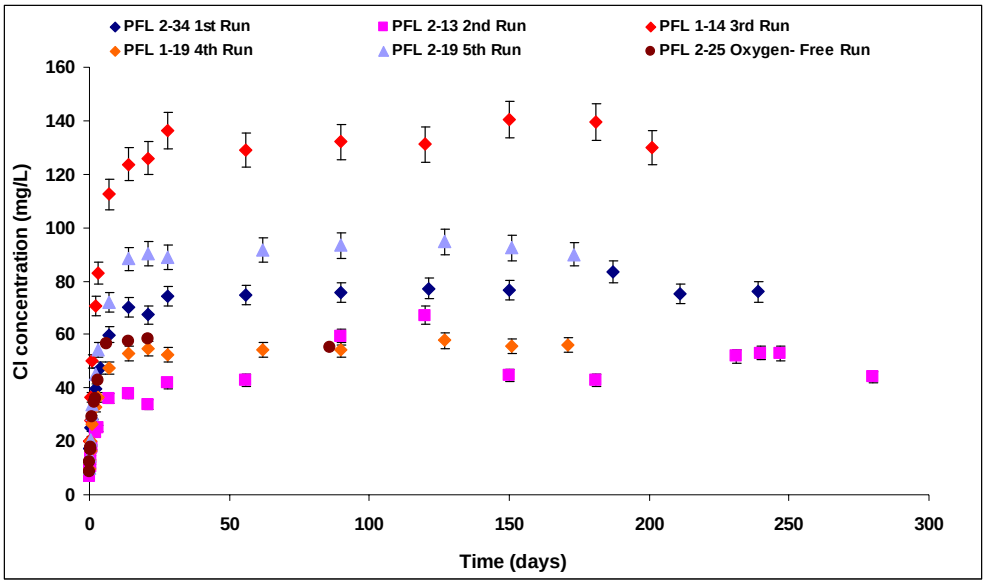

Figure 7. Chloride Concentration in Solution versus Time for the Six Timed Diffusion Experiments

The error bars indicate an analytical uncertainty of 5% in the measured Cl^- concentration.

In Figure 6, the five breakthrough curves (except experiment #2,) exhibit a similar trend, whereby the concentration of Cl^- increased rapidly at early time, and then began to plateau as steady state was approached (see Figure 7). In other words, the curves are not consistent with a differential process whereby they would normally show an asymptotic approach to the final value.

Another similarity between experiments was the length of time (28 days) required for the constituents of the pore fluid from each section of rock to approach steady-state (with the exception of experiment #2).

At 28 days the Cl^- concentration measured for diffusion experiment #2, was thought to have achieved steady-state at 44 mg/L. However, at 90 and 120 days, values of 59 and 67 mg/L were measured respectively. These values were beyond the range of analytical uncertainty (± 5%). One possible explanation may be due to microfracturing within the rock core caused by unloading stresses. These microfractures may have caused fluid inclusion leakage and/or the release of additional pore

fluids, thereby resulting in the initial increase in Cl^- concentration observed at early time followed by a steady incline in concentration seen over the remaining term of the experiment. However, the source of the elevated Cl^- concentrations cannot be determined with certainty.

A major difference between the five experiments is the final Cl^- concentration obtained at steady state. Steady state Cl concentrations range between 43 and 139 mg/L, which was unexpected based on the visual homogeneity of the core, and the proximity (at the site) of the two cored boreholes (PFL 1 and PFL 2). In addition, the rate at which Cl^- concentrations increased at early times also varied, generating different slopes for each of the five, timed diffusion experiments.

In the final solutions sampled from each of the timed cells, additional measurements were made including: cation and anion concentrations, pH and alkalinity values). The results from both the timed and closed cells are presented in Table 1.

Table 1. Steady-State Chemical and Isotopic Data From the Out-diffusion Experiments (Timed and Closed)

Element Conc. (mg/L)	1st Exp. Timed	1st Exp. Closed	2nd Exp. Timed	2nd Exp. Closed	3rd Exp. Timed	3rd Exp. Closed	4th Exp. Timed	4th Exp. Closed	5th Exp. Timed	5th Exp. Closed	De-oxygenated timed	De-oxygenated Closed
Anions												
Fluoride	1.8	1.7	Nd	Nd	2.6	1.7	2.6	1.8	1.6	1.7	Na	Na
Chloride	76	73	44	82	130	103	56	72	90	127	55	88
Bromide	6.8	Nd	38	5	Nd	Nd	3	Nd	Nd	Nd	Nd	Nd
Sulphate	10	9.8	Nd	22	13	12	13	10	10	12	16	25
Cations												
Calcium	150	148.5	140	160	160	158.5	120	130	130	160	78	100
Magnesium	0.29	0.26	0.13	0.20	0.33	0.39	0.27	0.31	0.38	0.32	0.190	0.190
Potassium	4.4	4.1	1.6	2.4	4.1	3.9	3.4	3.5	3.3	3.6	3.2	3.1
Sodium	15	13.5	11	17	15	13	12	14.5	14	16	9.6	12
Strontium	0.48	0.45	.044	0.42	0.32	0.39	0.26	0.31	0.42	0.49	0.25	0.38
Electro Neutrality (E.N.%)	33.23	39.54	24.67	15.5	32.67	38.06	40.32	26.63	34.88	31.96	9.11	26.28
pH	7.00	6.80	6.75	6.77	6.25	6.79	7.06	6.78	6.91	6.99	7.01	6.95
Alkalinity	188	136	292	420	44	72	92	216	76	72	208	32

The analytical results show that pore fluid chemistry, particularly chloride, is variable over small distances within the host-rock. However, the elemental composition is characteristic of deep shield brines. The waters are Ca-Cl dominated, with trace amounts of Sr and Br.

Table 1 shows two important characteristics. The first being the electro-neutrality (E.N. %) or charge balance data. All the charge balance data (with the exception of the de-oxygenated, timed cell results) exhibit a value greater than the accepted ±10% error normally associated with electro neutrality calculations. The charge balance inequality may be related to the abundance of Ca in the groundwater system, which may have precipitated and therefore was unable to be removed from solution by filtration. Another explanation may be due to the presence of some other ion that was not originally analyzed or an error in the alkalinity measurement as demonstrated by the difference in magnitude between alkalinity values (32-420). Due to the possibility of inaccurate alkalinity readings, bicarbonate could not be properly calculated, thus causing large percent errors. However, this does not impact the accuracy of the cation and anion concentrations (particularly the Cl^- concentrations).

4.1.2 Closed Cells

The closed cells were sampled once, after 5 months of reaction when the results of the timed experiments indicated that steady-state conditions had been reached. Analyses included cation and anion concentrations, pH, and alkalinity. The closed cell results are also provided in Table 1 for comparison with respect to the timed cells results. The objective for having a closed cell (i.e. a duplicate diffusion experiment) was to evaluate the precision of the out-diffusion method and the homogeneity of the core. Given that each pair of cores (timed and closed) should be mineralogical and chemically similar, final concentrations were expected to be comparable.

4.1.3 Repeat Diffusion Experiment

To ensure that steady-state conditions had been reached after 5 months, and that all the accessible Cl^- had been removed, a repeat diffusion experiment was conducted using the cores from diffusion run #1 (timed). The repeat experiment was conducted using the same methodology as outlined in Chapter 3.2, with one exception; the experiment was terminated after three months. The results indicated that leachable Cl^- concentrations remained relatively constant at about 3.2 mg/L (see Figure 8), an order of magnitude lower compared to the initial diffusion run which had a steady state Cl^- concentration of about 76 mg/L (Figure 7). This experiment confirmed that virtually all the accessible pore fluids had been successfully removed during the initial out-diffusion experiment.

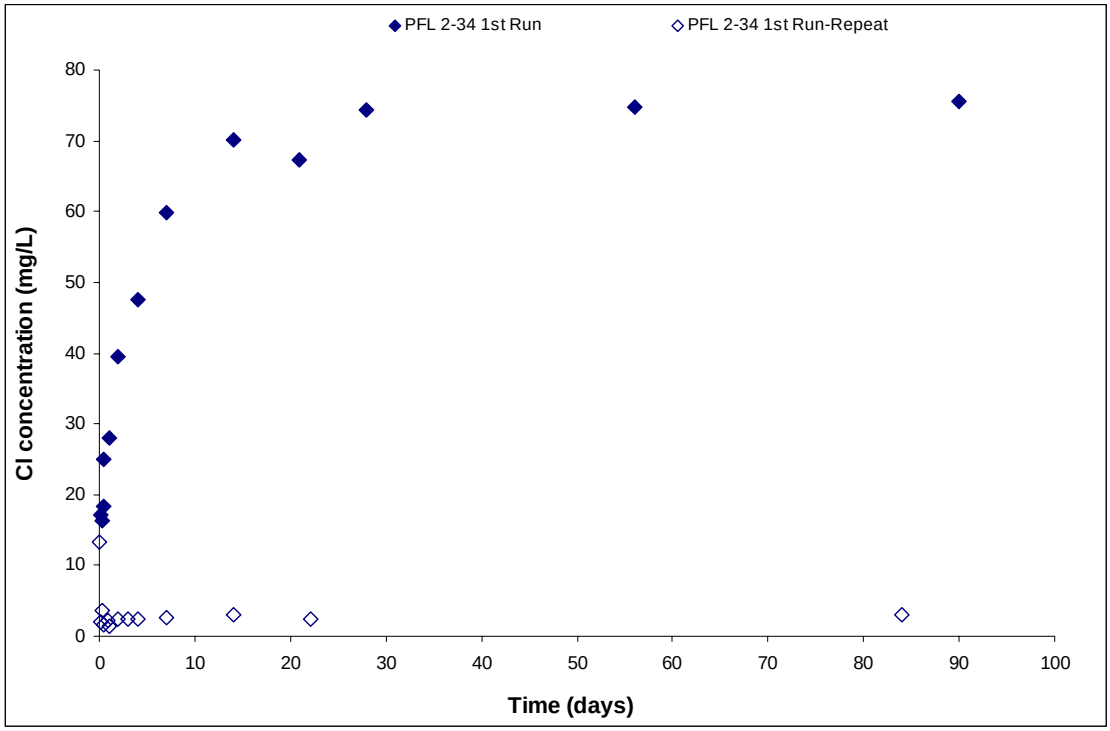

Figure 8. Cl^- Concentration vs. Time for Diffusion Run #1 and the Repeat Experiment

4.1.4 Surface Cl Estimation

In order to estimate the amount of chloride, which may have diffused out of the core (towards the outer surface) during shipment to the laboratory, the aluminium foil in which each core was wrapped was removed and rinsed with doubly de-ionized water. The weight of rinse water used was recorded, and the rinse solution analyzed for chloride concentration (Table 2). This concentration, albeit small, as is the case for diffusion experiment #5 (timed), is considered significant when trying to evaluate a representative value for pore fluid salinity.

Table 2. The Calculated Weight of Cl- Removed from the Aluminium Foil from Each Core Section

Diffusion Experiment	Wt. of Ultrapure Water Added (g)	Cl concentration (mg/L)	Calculated Wt. of Cl Removed from Foil (mg)
First Exp. (Timed)	10.04	13.48	0.135
First Exp. (Closed)	17.24	4.56	0.0778
Second Exp. (Timed)	14.77	3.00	0.0443
Second Exp. (Closed)	16.14	3.10	0.0500
Third Exp. (Timed)	7.96	3.01	0.0239
Third Exp. (Closed)	15.90	0.93	0.0147
Fourth Exp. (Timed)	16.79	1.22	0.0204
Fourth Exp. (Closed)	15.88	2.09	0.0325
Fifth Exp. (Timed)	16.51	0.88	0.0145
Fifth Exp. (Closed)	16.26	1.85	0.0300
De-oxygenated (Timed)	13.71	2.76	0.0378
De-oxygenated (Closed)	12.92	NA	NA

The amount of Cl^- removed from the aluminium foil was assessed to determine if there was a correlation between the amount of Cl^- rinsed from the aluminium foil, and the concentration of Cl^- measured in solution after 1 hour of diffusion. The results for the five timed experiments are shown in Table 3.

Experiment #1 had the highest amount of Cl^- initially removed from the aluminium foil, and the highest Cl^- concentration after 1 hour of reaction. However, experiment #2 had the second highest Cl^- concentration removed from the aluminium foil, yet this cell had the lowest Cl^- concentration in solution after one hour of reaction. Conversely, the highest steady-state value for Cl^- was observed in experiment #3, which had the third lowest amount of Cl^- removed from the foil. These finding suggest that there is no correlation between the amount of Cl^- removed from the foil and the Cl^- concentration observed after 1 hour of reaction, or at steady-state.

Table 3. The Relationship Between the Amount of Cl^- Removed from the Aluminium Foil and Concentrations Obtained after 1 Hour and at Steady-State

Diffusion Experiment	Calculated Wt. of Cl^- Rinsed from Foil (mg)	Cl^- Concentration After 1 Hour of Reaction (mg/L)	Cl^- Concentration at Steady-State (mg/L)
First Exp. (Timed)	0.135	18.3	75
Second Exp. (Timed)	0.0443	6.98	43
Third Exp. (Timed)	0.0239	20.16 after 3 hours (no 1 hour sample taken)	139
Fourth Exp. (Timed)	0.0204	9.38	55
Fifth Exp. (Timed)	0.0145	10	92
De-oxygenated (Timed)	0.0378	8.65	56.73

4.1.5 Quality Assurance

There are noticeable discrepancies in the Cl^- concentrations obtained at steady-state from each set of diffusion experiment. These differences may be attributed to natural uncertainties such as heterogeneity within the host rock or experimental uncertainties that may be associated with analytical error, improper design and/or implementation. To assess whether the difference in Cl^- concentration is attributed to analytical error, the accuracy of the IC method was evaluated as described below.

4.1.5.1 Accuracy of the IC Method for Cl Analysis

In order to evaluate the accuracy of the ion chromatograph method for Cl^- measurements, a set of samples was analyzed using two different ion chromatograph systems, a DX600-OH and DX600-CO_3 (Table 4). A graphical representation of the data presented in Table 4 is shown in Figure 9. The percent difference between the two calibration methods is illustrated in Table 4. With the exception of the calibration standard ICSTD_1000x, all of the expected Cl^- concentrations are within a ±10% difference. Therefore, irrespective of the ion chromatograph method used, the difference in concentration is negligible, implying that the difference in Cl^- concentration cannot be attributed to the IC method used.

Table 4. The Calculated Percent Difference Between the Cl^- Concentrations Obtained Between the Two Ion Chromatograph Methods

Calibration Method	Calibration Standards	Expected [Cl] DX600-OH	Actual [Cl] mg/L	Area of Chloride Peak µS*min	Percent Difference %
DX600-OH System	ICSTD_1000x	0.2	0.188	0.047	-11.6
	ICSTD_100x	2	1.99	0.498	7.13
	ICSTD_40x	5	4.989	1.250	3.49
	ICSTD_20x	10	9.09	2.483	-8.15
DX600-CO_3 System	ICSTD_1000x	0.2	0.2127	0.042	11.6
	ICSTD_100x	2	1.8576	0.363	-7.13
	ICSTD_40x	5	4.8206	0.941	-3.49
	ICSTD_20x	10	9.8963	1.932	8.15

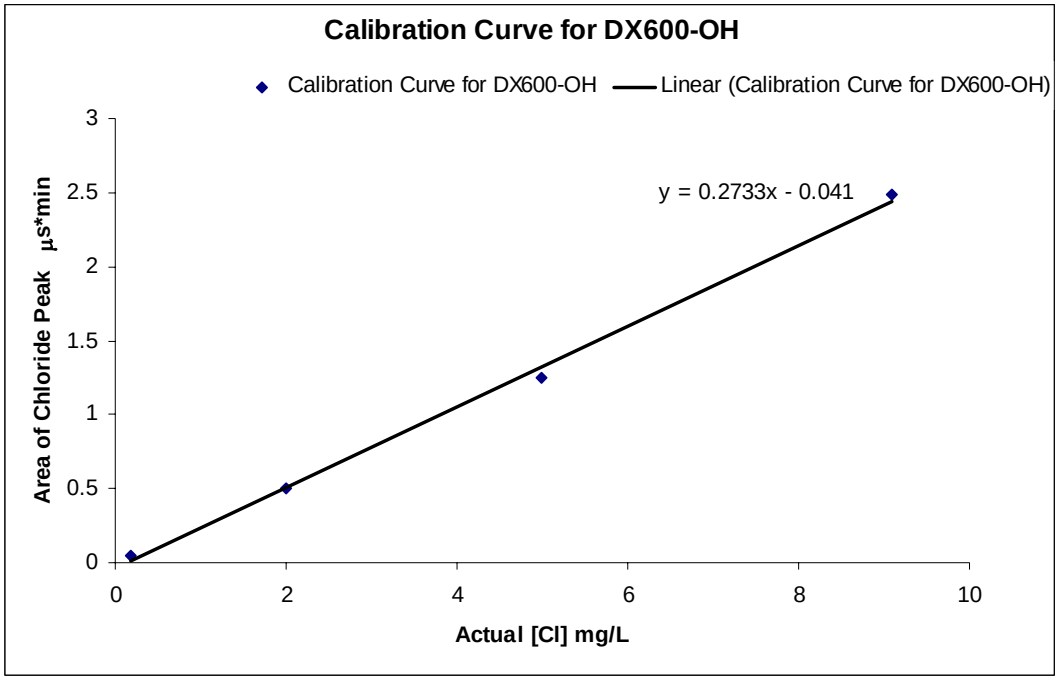

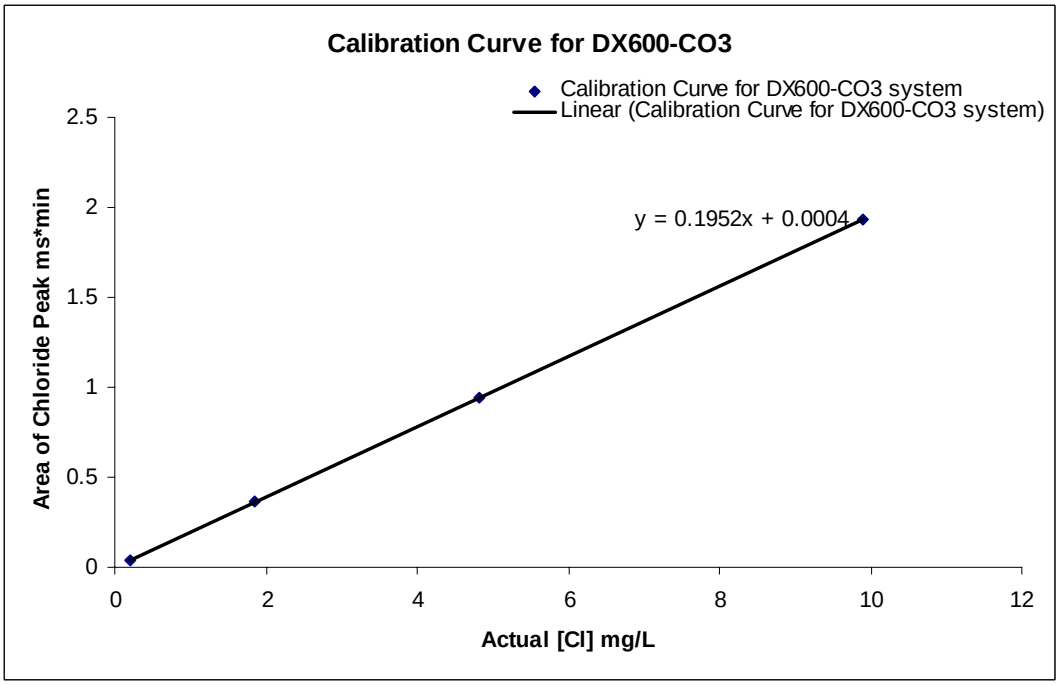

Figure 9. Calibration Curves for the Different ion Chromatograph Techniques used a) DX600-OH b) DX600-CO3

4.1.5.2 Consistency of Water: Rock Ratio (Timed Cells)

As documented in Table 2, only small sample volumes (less than ≈ 4 mL) were removed from the reaction cells at each sampling. The purpose was two-fold: i) to maintain stable water to rock ratios for the duration of the experiment; and ii) to ensure that the core remained completely submerged in the reaction cell for the duration of the experiment. By maintaining nearly constant water to rock ratios, the variation in Cl concentration measured in solution (between runs 1 through 5) is not likely the result of increased concentration due to the removal of water. As demonstrated in Table 5, water to rock ratios remained relatively constant throughout the duration of the experiments and was only marginally lower at the end of the experiments, with respect to starting ratios.

Table 5. Comparison Between Initial and Final Water: Rock Ratios

Diffusion Experiment	Wt. of Water Initially Added (g)	Wt. of Core (g)	Initial Water:Rock	Wt. of Water Removed (g)	Wt. of Water Remaining (g)	Final Water:Rock
First Exp. (Timed)	301.11	1128.8	0.267	7.19	293.92	0.260
First Exp. (Closed)	287.89	1125.43	0.255	0	287.89	0.255
Second Exp. (Timed)	299.77	1076.3	0.279	5.65	294.12	0.273
Second Exp. (Closed)	315.48	1071.19	0.294	0	315.48	0.294
Third Exp. (Timed)	300.57	1133.12	0.265	5.42	295.23	0.260
Third Exp. (Closed)	292.61	1144.01	0.255	0	292.61	0.255
Fourth Exp. (Timed)	313.37	1113.12	0.281	5.34	308.03	0.277
Fourth Exp. (Closed)	300.35	1065.65	0.282	0	300.35	0.282
Fifth Exp. (Timed)	321.24	1075.55	0.299	5.24	316.00	0.294
Fifth Exp. (Closed)	325.15	1076.11	0.302	0	325.15	0.302
De-oxygenated (Timed)	318.71	1078.68	0.295	4.09	314.64	0.292
De-oxygenated (Closed)	319.25	1054.86	0.303	0	319.25	0.303

4.2 CRUSH AND LEACH EXPERIMENTS

Several different crush and leach methods were conducted to determine the maximum amount of Cl^- released from both pore fluids (accessible) and fluid inclusions (non-accessible unless ruptured). An initial experiment was performed on core from a test borehole taken from the URL. The remaining experiments used core from borehole PFL 2 (sections -14, -15, -33 and –34). The first method was a timed crush and leach experiment. That is, various grain sizes were leached until steady-state Cl^- concentrations were obtained (refer to Chapter 3.3 for further details). The purpose for conducting the timed leach experiments was to corroborate the findings by AECL, which suggested that all the leachable Cl^- could be removed within 20 minutes and was not a function of the water to rock ratios (AECL, 1987). The second method involved leaching various grain sizes over an arbitrary time interval of 24 hours. This method was used to determine if the amount of leachable Cl was a function of grain size (i.e. Cl increased as the grain size decreased) rather than time.

The third and final method was a progressive crush and leach. The purpose of which was two fold. First, to determine the impact of water to rock interactions at various grain sizes and secondly, to determine the possible impact of fluid inclusion leakage on pore water salinity. Further details regarding the methodology are provided in Chapter 3.3.

The results from the crush and leach experiments are plotted in Figure 10, and are tabulated in Tables A2-A4 of Appendix A. As expected the results from Figure 10a demonstrate that as the grain size decreases, the amount of leachable Cl increases.

Figures 10b and c illustrate three different grain sizes leached at various water to rock ratios (i.e. either 1:1 or 2:1). The results show that after 20 minutes of leaching the concentrations of Cl become relatively constant, thus corroborating with the findings from AECL, (1987) that the amount of leachable Cl is a function of grain size and leach time (20 minutes) and not the water to rock ratio.

The results from the progressive crush and leach experiment are presented in Figure 10e, which also shows how successive leaching can cause an increase in Cl^- concentration. The slight increase in concentration observed with a decrease in grain size is considered to be the result of fluid inclusion leakage, thereby releasing slightly more saline fluids into solution. However, it should be noted that concentrations obtained through progressively leaching the rock core were not significantly different than those obtained by using the out-diffusion method. As a result, fluid inclusions (within the crystalline rock from the URL) are not suspected to be large contributors to pore fluid salinity.

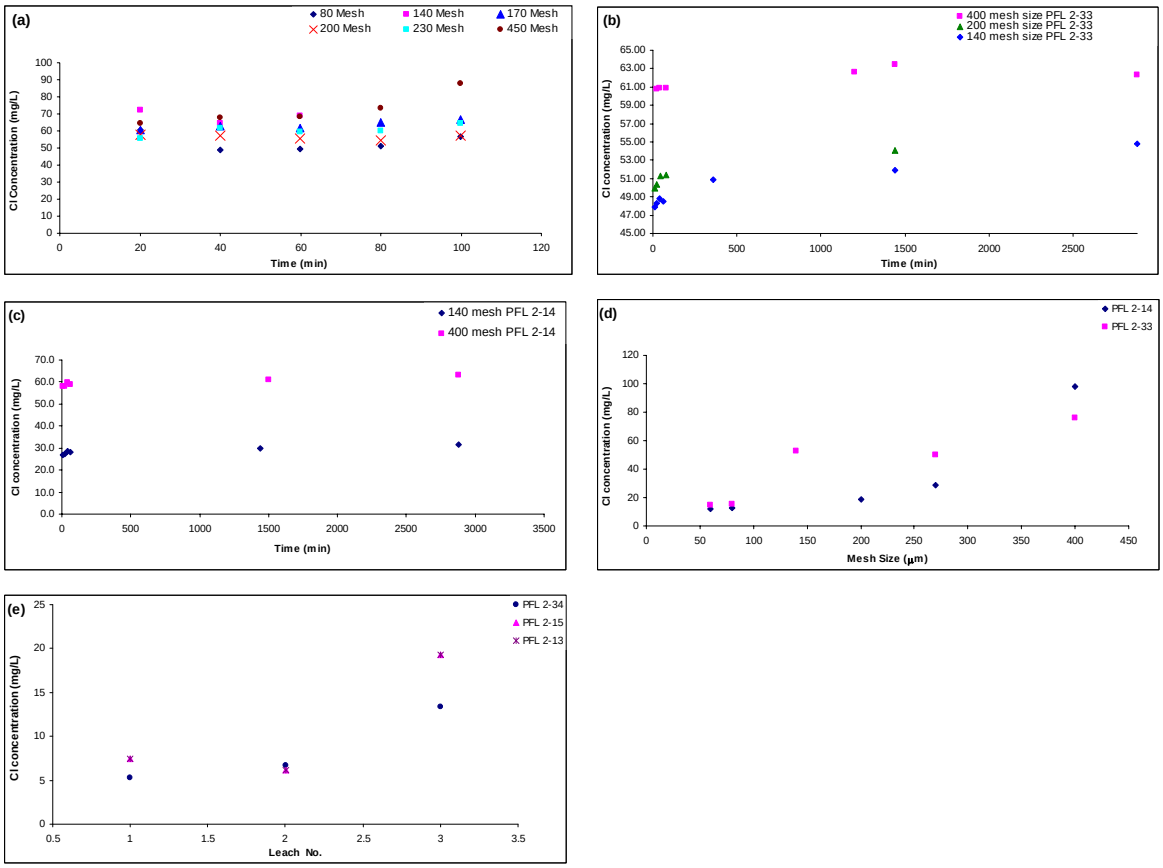

Figure 10. Crush and Leach Results

a) Crush and leach data from the test borehole, b) the timed leaching experiment results from borehole PFL 2 (PFL 2-33) c) leaching results from borehole (PFL 2-14), d) the Cl^- concentrations as a function of grain size, and e) progressive crush and leach results.

4.3 ISOTOPE ANALYSES

Water samples were taken from the diffusion and crush and leach experiments in order to analyze for the isotopic ratios of ^{18}O, ^{2}H, ^{37}Cl and ^{87}Sr. The purpose of the isotopic analyses was to determine the origin(s) of the pore fluid, the extent of water-rock interaction and other geochemical processes that may be useful when assessing the suitability of crystalline rock environments for radioactive waste disposal. The results from these findings are presented in the following chapters.

4.3.1 $\delta^{18}O$ and $\delta^{2}H$

Isotopically depleted water with an ^{18}O and ^{2}H signature of -113.4‰ and -917.51‰ respectively, was added to diffusion experiments 4 and 5 (see Figure 11). The purpose for using such isotopically depleted water was to calculate the original isotopic composition of the pore fluid based on an observed isotopic shift that would occur when depleted water was mixed with the isotopically heavier pore fluid.

The results indicated that ^{18}O became more depleted (–116.54 and –118.94 ‰), whereas ^{2}H became more enriched (-895.29 and –896.12‰) with respect to the GMWL and the initial isotopic composition of the water (added to the cell) (Table 6). When the results are plotted on an ^{18}O and ^{2}H graph the sample data (with the exception of diffusion run #5, timed) plots above and to the left of the GMWL, which is a diagnostic property of shield brines (Frape and Fritz, 1982). However, it should be noted that the ^{2}H values remain relatively constant whereas the ^{18}O values vary significantly. The same results were found in studies conducted in the Massif Centrale of France. Kloppmann et al., (2002) attributed the isotopic shift to be the result of an exchange reaction between the oxygen isotope and a CO_2 dominated gas. However, groundwaters within the Canadian Shield are typically low in pCO_2 concentrations, although concentrations of HCO_3 within the granitic rock used for the present out-diffusion experiment were elevated. Another possible explanation for the depleted ^{18}O and enriched ^{2}H

values may be due to water-rock interactions, more specifically, an exchange reaction between groundwater and the dominant mineral phase.

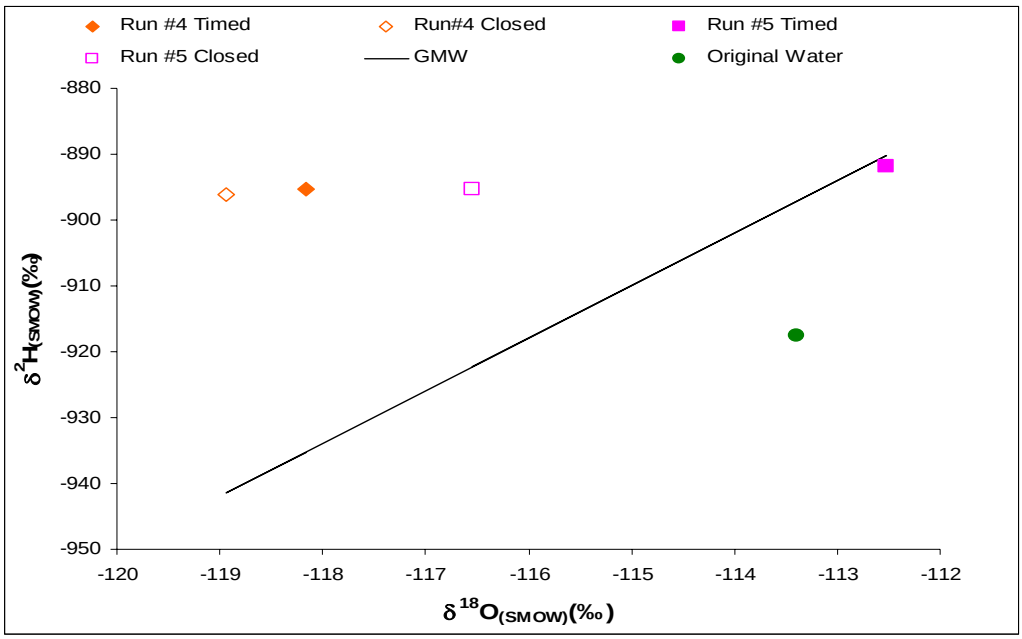

Figure 11. $\delta^{18}O$ and $\delta^{2}H$ Values Obtained from Diffusion Runs #4 and 5

These are relative to the isotopic signature of the original water added to the cell and the GMWL

In order to estimate the original isotopic composition of the pore fluid a mass balance approach was used whereby,

$$\delta^{18}O_{final} = n_b\delta^{18}O_b + n_p\delta^{18}O_p \quad (8)$$

$\delta^{18}O_{final,}$ $\delta^{18}O_b$ and $\delta^{18}O_p$ represent the isotopic composition of the residual solution, bulk solution and pore water respectively. The symbols nb and np correspond to the fraction of the bulk solution and pore water respectively within each cell (see example calculation in Appendix A). The same equation is also used to estimate the original $\delta^{2}H$ composition.

Due to the extreme isotopic signatures found in the final solution, a reasonable ^{18}O and ^{2}H value could not be calculated for the pore water (see sample calculation in Appendix A). In other words, the volume of pore fluid relative to the bulk solution was too small. As a result, the isotopic composition of the bulk solution (originally added to the cells) concealed the isotopic signature of the pore fluid. Consequently, the out-diffusion experiment was not successful in back calculating the ^{18}O and ^{2}H signatures of the pore fluid.

Table 6 lists the ^{18}O and ^{2}H signatures from borehole seepage and drill waters sampled directly from open boreholes (PFL 1 and PFL 2) within the URL. Seepage waters have ^{18}O and ^{2}H signatures ranging between – 10.6 to -16.05‰ and -10.55 to -39.74 ‰ respectively, which may also be representative of pore fluid signatures. However, to correctly identify the pore fluid signature using an out-diffusion experiment, larger quantities of pore fluid and its constituents would have to be extracted and analyzed.

Table 6. The Isotopic Signatures of Seepage and Drill Waters Sampled Directly from Open Boreholes Within the URL

Sample	^{18}O result	^{2}H result
inflow to PFL 2 zone 1	-10.67	-39.74
inflow to PFL2 zone 2	-11.57	-39.02
inflow to PFL 2 zone 2 (2 days later)	-11.41	-33.95
Seepage from original sloping borehole	-14.51	-14.1
inflow to PFL 1 zone 1	-14.63	-28.72
inflow to PFL 1 zone 2	-15.46	-14.32
inflow to PFL1 zone 2	-11.95	-36.23
inflow to PFL1 zone 2	-15.62	-10.55
inflow to PFL 2 zone 1	-12.16	-33.15
Seepage from original sloping borehole	-14.51	-14.93
inflow to PFL 2 zone 2	-11.92	-33.98
PFL 2A Potable Water	-8.2	-72.02
PFL-DEW A Drill Water	-8.73	-74.34

Table 6. The Isotopic Signatures of Seepage and Drill Waters Sampled Directly from Open Boreholes Within the URL

Sample	^{18}O result	^{2}H result
PFL-2 DEW B Drill Water	-8.45	-73.34
PFL 2-1 April	-12.09	-31.22
PFL 1-2 April	-15.91	-10.93
SMR April	-14.21	-13.34
PFL 2-1 May	-11.87	-24.58
PFL 2-2 May	-12.11	-33.03
PFL 1-2 May	-16.05	-11.17
SMR May	-14.02	-13.31

4.3.2 Chloride concentrations and Chlorine 37

The final solutions from each of the six diffusion runs were analyzed for ^{37}Cl and Cl^- concentration (Figure 12 and Table 7) in order to determine a) the $\delta^{37}Cl$ signature of the leached Cl^-, b) the heterogeneity of $\delta^{37}Cl$ signatures between diffusion runs, and its relation with Cl^- concentration, c) the source of the $\delta^{37}Cl$ signature and the effects of processes such as diffusion which may alter that signature, d) the possible relation between $\delta^{37}Cl$ values from the timed diffusion runs and the crush and leach experiments and e) any possible correlation between $\delta^{37}Cl$ results from the present study to historical data collected from the site.

The analytical data is scattered and shows a poor correlation between Cl^- concentration and ^{37}Cl, which does not provide enough evidence to suggest a single source or a mixing between end-members.

Based on the enriched isotopic signatures, these values exclude the possibility of a modern marine derived salinity. In addition, the stable chlorine isotope values lie within the range of igneous alkaline rocks (0.09 to 0.88‰), particularly those similar to other crustal samples.

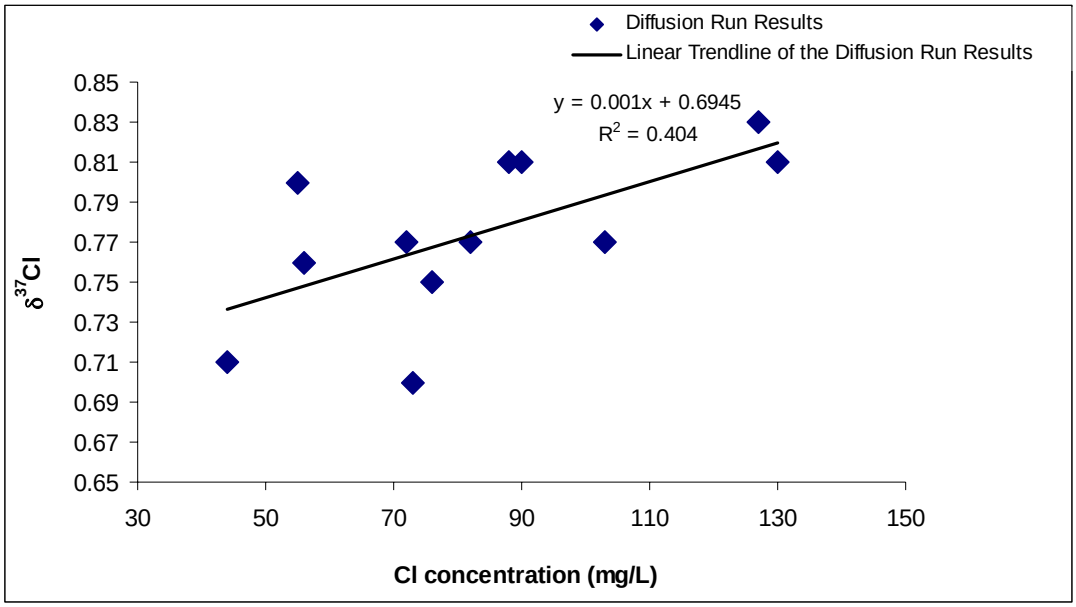

Figure 12. A plot of $\delta^{37}Cl$ vs. Cl Concentration from Each of the Six Diffusion Runs (Timed and Closed)

Figure 12 shows the variation in the $\delta^{37}Cl$ vs. Cl^- concentration, which were found to vary by as much as ±0.13, which lie outside the range of analytical uncertainty (± 0.1).

The heterogeneity in chemical composition ($\delta^{37}Cl$ and Cl^- concentration) measured between the various diffusion experiments (Figure 12) was suspected to be the result of variations in pore fluid salinity and/or porosity. In an attempt to determine the validity of this hypothesis, accurate calculations of pore fluid salinity were required, because it was suspected that there was a direct correlation between the degree of pore fluid salinity and porosity, therefore accurate porosity measurements were required.

Porosity measurements were conducted on each of the twelve cores (six pairs), as described in Chapter 3.2.6, in order to determine the actual pore fluid salinity. An average porosity value of about 0.003 was obtained for each core section and used in each of the pore fluid salinity calculations (a sample calculation is provided in Appendix A). As a result, the variability in pore fluid salinity (shown in Table 7) cannot be attributed to large variations in porosity.

Table 7. ^{37}Cl, Cl Concentration and Pore Fluid Salinity Results

Diffusion No.	^{37}Cl (‰)	Cl concentration (mg/L)	Pore Fluid Salinity (g/L)
1st Run (Timed)	0.75	76	7.51
1st Run (Closed)	0.7	73	6.91
2nd Run (Timed)	0.71	44	4.53
2nd Run (Closed)	0.77	82	8.95
3rd Run (Timed)	0.81	130	12.9
3rd Run (Closed)	0.77	103	9.88
4th Run (Timed)	0.76	56	5.9
4th Run (Closed)	0.77	72	7.59
5th Run (Timed)	0.81	90	9.96
5th Run (Closed)	0.83	127	14.2
De-oxygenated (Timed)	0.8	55	6.02
De-oxygenated (Closed)	0.81	88	9.86

Notes: Samples obtained from the final solution of each diffusion run.

When the chlorine isotope data was plotted against the calculated pore fluid salinity (Figure 13), a trend, similar to that shown in Figure 12 (but with a slightly better correlation) was observed. A general increase in $\delta^{37}Cl$ values was associated with an increase in pore fluid salinity. Based on these results, there may be a correlation between pore fluid salinity and $\delta^{37}Cl$ composition.

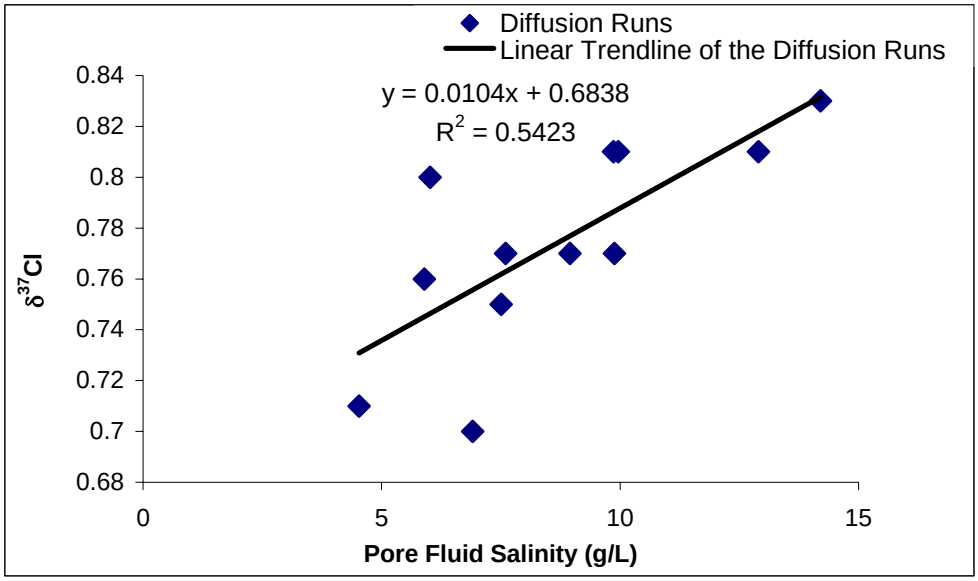

Figure 13. Pore Fluid Salinity Measurements vs. the Isotopic Composition of Chloride

Based on studies such as those by Sie and Frape, (2002), it was suspected that $\delta^{37}Cl$ values may be related to but are not exclusively controlled by the mineralogical composition of the cores (i.e. intense water-rock interaction), particularly the percent of dark minerals such as biotitic and its alteration product, chlorite (Orphan, 1997). As a result, a mineralogical investigation (thin section analysis) was conducted using core segments from each of the diffusion experiments (see Table 8 and Figure 14).

Table 8. The Relative Cl Concentration, Mineralogical Description, Percent Biotitic, $\delta^{37}Cl$ and $\delta^{87}Sr$ Values from Each Diffusion Run

Chemical Analysis	Sample ID									
	3rd Run Timed	3rd Run Closed	5th Run Closed	5th Run Timed	1st Run Timed	1st Run Closed	4th Run Closed	4th Run Timed	2nd Run Closed	2nd Run Timed
Cl concentration (mg/L)	130	103	127	90	76	73	72	56	82	44
Sr concentration (mg/L)	0.32	0.39	0.49	0.42	0.48	0.45	0.31	0.26	0.38	0.25
Mineralogical description	NA	More plag than biotite	Biotite is conc. in certain areas	Biotite is conc. in areas	Big plag, less biotite	Big plag. less biotite	More disseminated biotite, some big plag	More disseminated biotite, some big plag	Qtz. dominated Big biotite-mica	NA
% biotite, chlorite and opaques	NA	8	15	18	3	3	7	5	2	NA
$\delta^{37}Cl$	0.81	0.77	0.83	0.81	0.75	0.70	0.77	0.76	0.77	0.71
$^{87}Sr/^{86}Sr$	0.7918	0.7979	0.7727	0.7734	0.7708	0.7724	0.7997	0.7959	0.7665	0.7657

The results show that as the concentration of biotitic and other dark minerals increases (see Figure 14 and 15), so does the relative ^{37}Cl value, thereby supporting the findings from Orphan, (1997). As a result, small heterogeneities in the bulk mineral composition of each rock core can significantly change the chemical and isotopic composition of the pore fluid. This is considered to be the case in old rocks (such as crystalline rocks) that have had time to undergo exchange reactions with the dominant mineral phase.

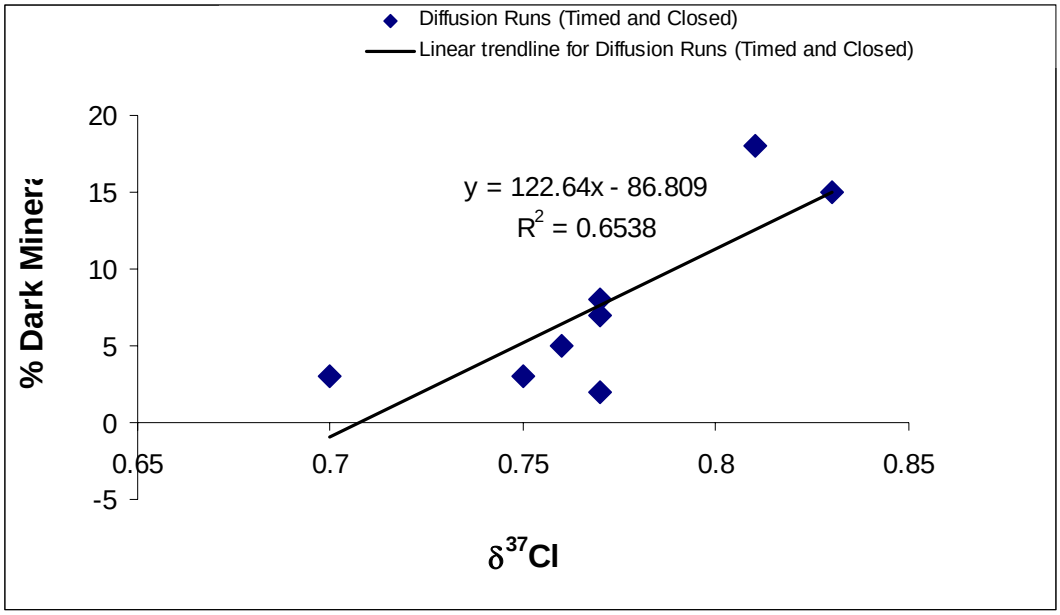

Figure 14. Percent of Dark Minerals (biotite, chlorite and opaques) Versus $\delta^{37}Cl$ Values Obtained from Each Diffusion Run

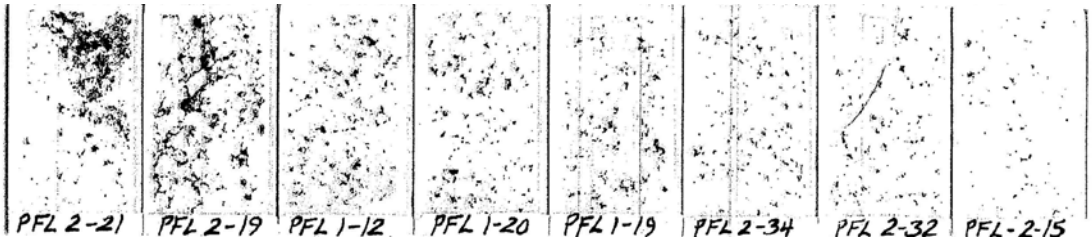

Figure 15. Petrographic Slides from Each of the Diffusion Experiment

Expect run #2 timed and run #3 timed due to insufficient samples), which exhibit a variation in the relative percent of dark minerals.

4.3.3 Strontium concentrations and $^{87}Sr/^{86}Sr$ analyses

Strontium has become useful for determining the influence of water-rock interaction on the chemical composition of groundwater, specifically, the dissolution of various mineral phases and their control on the isotopic signature of the pore fluid (McNutt, 1984). Due to the geochemical coherence of Sr and Ca, the relationship between these minerals can also be used in establishing the source(s) of Sr

within a groundwater system. In other words, the origin of the Sr will reflect the genesis of Ca in the brine (McNutt, 1984, Franklyn et al., 1991).

The analytical data shown in Table 8 also represents the $^{87}Sr/^{86}Sr$ ratios, and concentrations obtained from the five sets of diffusion experiments. The results illustrate significant variation in isotopic compositions (0.765 to 0.799), which exceed the analytical uncertainty for Sr, 0.0003 or 2σ. In addition, the isotopic values for Sr are much greater than those found in previous studies conducted on other Canadian Shield Brines (0.707 to 0.755) (McNutt et al., (1990); Franklyn et al., (1991)). Figure 16 (a) demonstrates $^{87}Sr/^{86}Sr$ ratios from a typical crystalline rock environment (felsic rock from the Eye-Dashwa pluton), which demonstrates a correlation between the $^{87}Sr/^{86}Sr$ signature and plagioclase. In addition, the more enriched ^{87}Sr values are in agreement with K-feldspar (Franklyn et al., 1991). Figure 16 (b) demonstrates how the ^{87}Sr values over time are dependent upon the minerals Rb/Sr ratio, and that groundwaters highly enriched in ^{87}Sr values may be attributed to equilibrium with K-feldspar and/ or muscovite (McNutt et al., 1990).

Such large deviations between the isotopic signatures obtained from the current study versus those in Figure 16 suggest that even small heterogeneities in the host rock composition can have significant impacts on the isotopic signature of the pore fluid, and that differences in heterogeneity can exist over small distances within the wall-rock (as shown based on the chemistry results between boreholes PFL 1 and PFL 2).

Based on the isotopic results from the out-diffusion experiments (Table 8), the pore fluid signatures appear to have equilibrated with mineral phases rich in Rb such as K-feldspar or mica. However, it should be noted that the isotopic signature of the pore water is controlled by the rate of mineral dissolution (see Table 9). As a result, minerals such as muscovite, which have an extremely slow dissolution rate, must be present in large quantities or control dissolution in order to cause an isotopic shift in pore fluid composition.

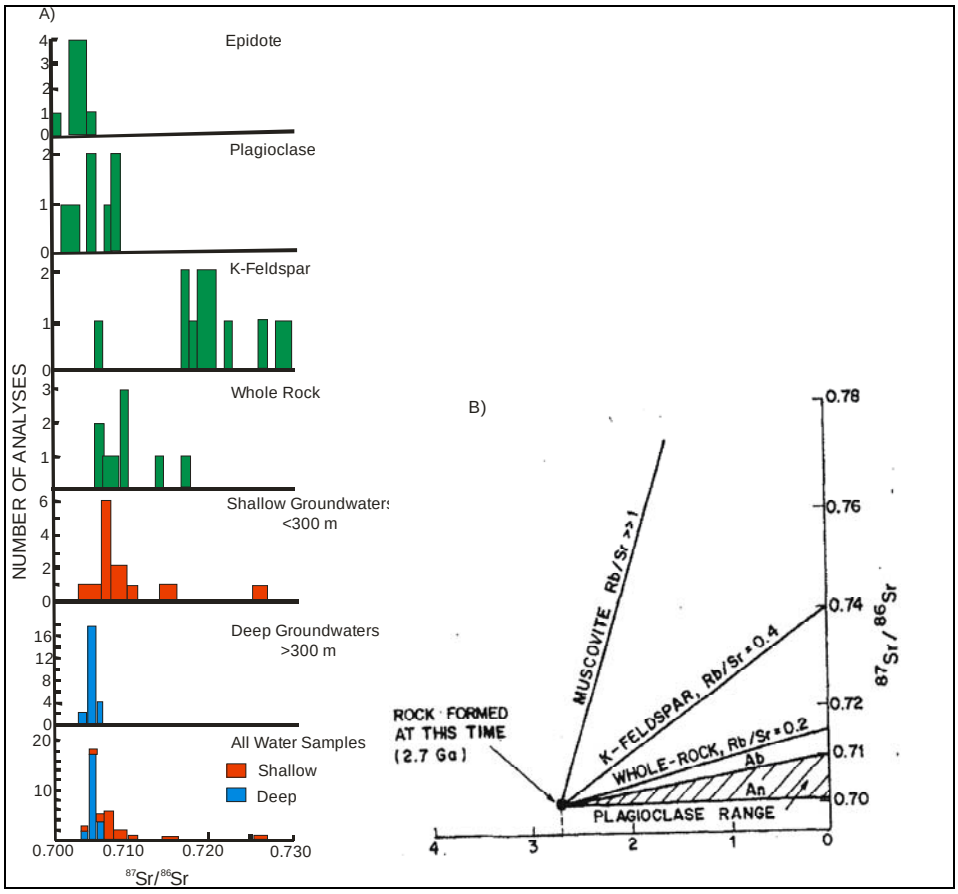

Figure 16. $^{87}Sr/^{86}Sr$ Signatures in Groundwater

a) $^{87}Sr/^{86}Sr$ signatures from groundwater, dominant mineral phases and whole-rock analyses taken from a typical crystalline rock environment (Franklyn et al., 1991) b) $^{87}Sr/^{86}Sr$ ratio changes with time as a function of the dominant mineral phase present (McNutt et al., 1990).

Table 9. Dissolution Times for Dominant Mineral Phases and Their Associated $^{87}Sr/^{86}Sr$ Ratios (McNutt et al., 1990)

Mineral Phase	Time (years)	Relative Concentration of Rb and Sr [1]	$^{87}Sr/^{86}Sr$ (‰)
Muscovite	27,000,000	VH VL	>>1
K-Feldspar	520,000	M-H M-H	0.730 – 0.800
Albite	80,000	L M-H	0.710 – 0.725
Diopside	6,800	VL L	0.701 – 0.703
Anorthite	112	VL H	0.702 – 0.703

note: VH = very high L = low
H = high VL = very low

To determine whether muscovite or K-feldspar controlled the isotopic signature of diffusion experiments 1 through 5, a petrographic and whole-rock analysis was conducted on each core sample (timed and closed). The results are presented in Table 10, and demonstrate that unlike $\delta^{37}Cl$, ^{87}Sr is not controlled by the relative percent of dark minerals (see Figure 17). In addition, the whole rock data presented in Table 10, demonstrates that silicate and aluminum silicate minerals dominate the host rock. However, the ^{87}Sr signatures do not reflect equilibrium with quartz or muscovite. Therefore, pore fluid equilibrium with feldspars and their alteration products may be a more viable explanation for such highly enriched Sr signatures. This is in accordance with a similar study conducted by McLaughlin, (1997) which also found pore fluids from the Lac du Bonnet batholith to lie within the same isotopic range as those obtained from the present out-diffusion experiments (see Figure 18). Upon examination of the host rock and the isotopic analyses of the individual mineral grains, the present study provides evidence that pore fluids may have undergone equilibrium partitioning with K-feldspar (Figure 18).

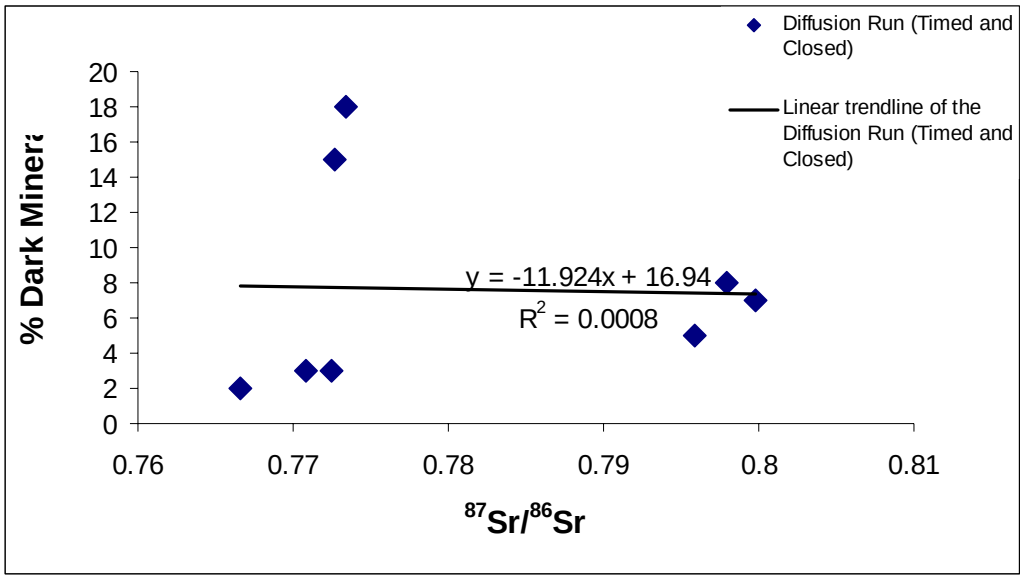

Figure 17. Percent of Dark Minerals Versus the $^{87}Sr/^{86}Sr$ Content from Each Core Segment (Timed and Closed)

Table 10. Whole-Rock Data

Sample No.	Oxide %											Sr (ppm)	Cl (ppm)
	SiO_2	Al_2O_3	CaO	MgO	Na_2O	K_2O	Fe_2O_3	MnO	TiO_2	P_2O_5	Cr_2O_3		
1st Run Timed	73.3	13.9	1.66	0.49	3.76	4.53	2.04	0.02	0.19	0.06	0.03	190	100
1st Run Closed	73.4	14.1	1.84	0.39	3.97	4.01	1.85	0.02	0.17	0.04	0.02	190	110
2nd Run Closed	76.4	12.4	1.22	0.11	3.23	4.57	1.96	<0.01	0.09	<0.01	0.03	170	90
3rd Run Closed	72.6	14.1	1.68	0.5	3.73	4.52	2.1	0.03	0.21	0.07	0.03	200	120
4th Run Timed	70.7	14.2	2.41	0.55	4.69	4.53	2.31	0.05	0.34	0.1	0.02	190	120
4th Run Closed	71.8	14.2	1.69	0.48	3.74	4.61	2.2	0.03	0.21	0.07	0.03	200	110
5th Run Timed	72.2	14.3	1.66	0.42	3.79	4.7	1.91	0.02	0.19	0.05	0.02	200	100
5th Run Closed	72.6	14.3	1.88	0.48	3.95	4.23	2.28	0.02	0.25	0.07	0.02	200	120
Measurable Uncertainty (%)	5	5	5	5	5	5	5	20	5	20	20	10	10

Notes: Values presented as percent oxide (%)
Run #2 and 3 timed did not have sufficient sample volumes for analysis and therefore are excluded from the table.

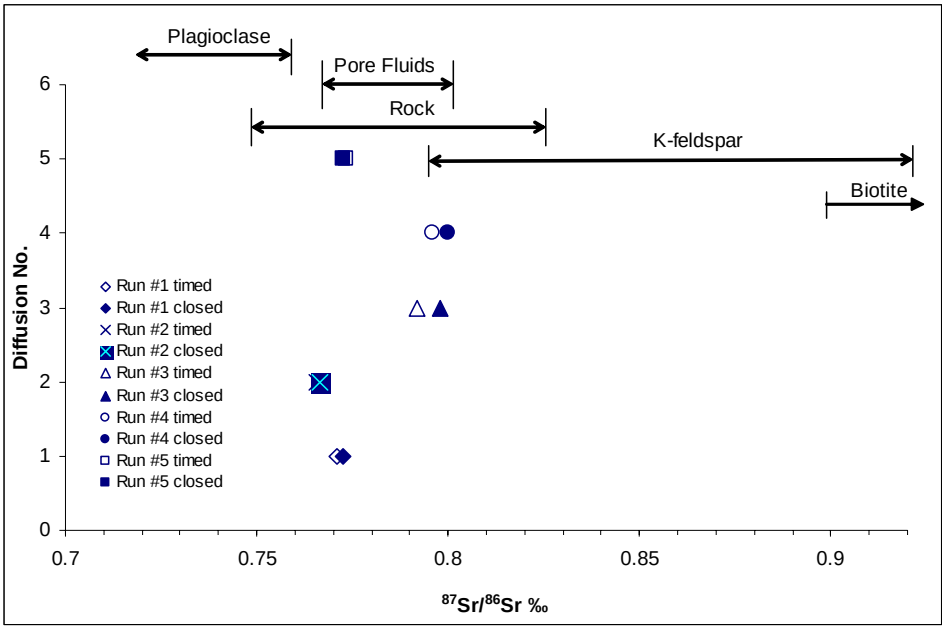

Figure 18. A Plot of the $^{87}Sr/^{86}Sr$ Ratios from the Out-diffusion Experiments

These values include the whole rock and mineral data from the Lac du Bonnet Batholith obtained by Li et al. (1989). The range labelled "pore fluids" is from McLaughlin, (1997).

The whole-rock data presented in Table 10 is shown graphically in Figure A1, and shows no relationship between the $^{87}Sr/^{86}Sr$ of the pore fluid and the concentration of MnO, MgO, TiO_2 and P_2O_5 in the host rock. Conversely, a negative relationship is observed between $^{87}Sr/^{86}Sr$ and SiO_2. The same correlations were observed when whole-rock data was plotted against Sr concentration. It should also be noted that, no significant trend was observed between $^{87}Sr/^{86}Sr$ and K_2O, Al_2O_3 or Fe_2O_3, which one might expect if feldspars or biotite were controlling the chemical composition of the pore fluid.

If we examine the $^{87}Sr/^{86}Sr$ ratio as a function of Sr concentration, then three distinct data sets become apparent (Figure 19). The first has an isotopic ratio ranging between 0.765 and 0.766, the second varies from 0.770 to 0.773, and the last plots at extremely high ^{87}Sr ratios, 0.795-0.800. Based on Figure 19 most diffusion experiments (timed and closed) were found to have similar isotopic signatures; however it should be noted that with the exception of diffusion experiment #5, most of the closed diffusion experiments had slightly more enriched $^{87}Sr/^{86}Sr$ signatures and slightly higher Sr concentrations relative to the timed cells. In addition, rock cores with a higher Sr concentration did not necessarily exhibit the highest $^{87}Sr/^{86}Sr$ ratios. Therefore, no correlation between the Sr concentration and the isotopic values were exhibited in Figure 19, which may suggest that mineralogical heterogeneities exist within the host-rock. Therefore, isotopic signatures may result from, 1) long-term pore fluid equilibrium with various mineral phases and/or their alteration products or 2) the presence of three isotopically distinct brines existing in close proximity to one another. Such a possibility is not unique to crystalline rock environments.

Due to their geochemical similarity, the relationship between Sr and Ca was examined to help determine if more than one groundwater system was present within the host-rock (Figure 20). Figure 20 shows a weak correlation between Sr and Ca, therefore the relationship between the geneses (i.e. the source) of the two elements cannot be successfully determined.

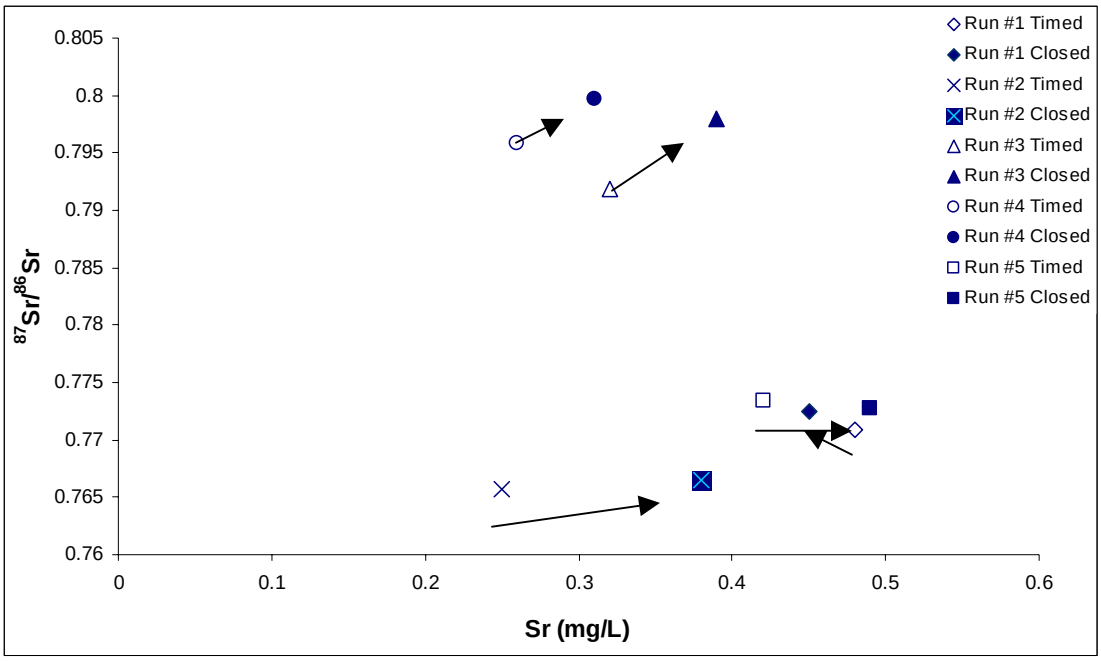

Figure 19. $^{87}Sr/^{86}Sr$ **Ratio vs. Sr Concentration, From Five Out-diffusion Pairs (Timed and Closed)**

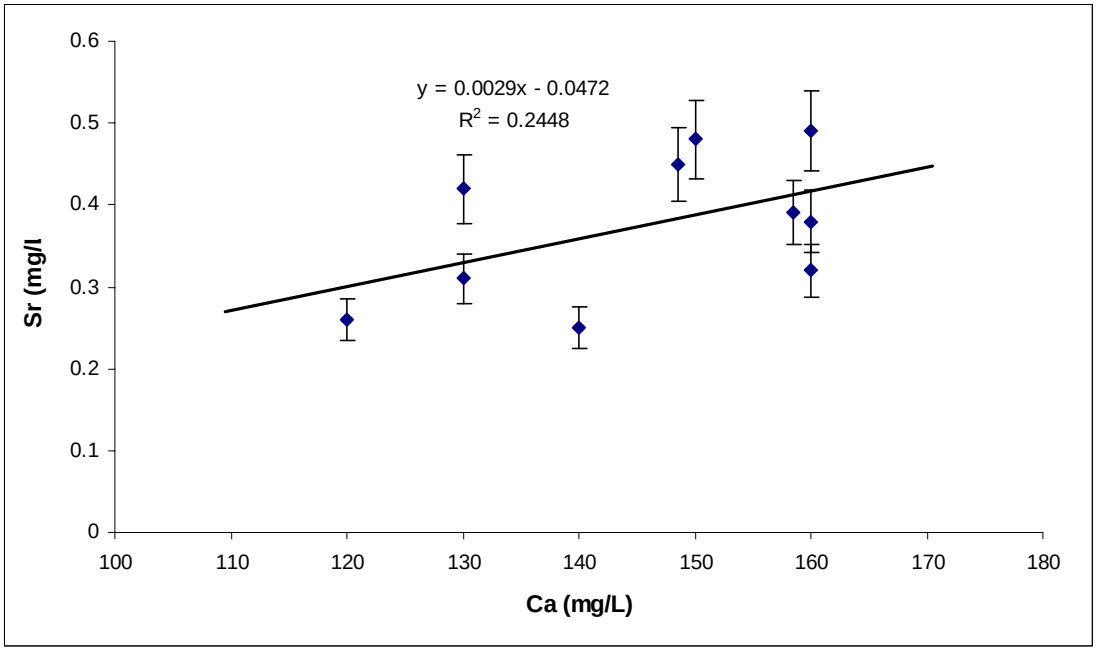

Figure 20. **The Sr vs. Ca Concentrations from Five, Out-diffusion Experiments**

In addition, to identify the presence of more than one chemically distinct group of groundwater within the host rock and/or to determine if mixing (between two or more chemically unique groundwaters) has occurred, Sr is plotted in an $^{87}Sr/^{86}Sr$ vs.1/Sr diagram, see Figure 21. This figure also shows no evidence that two groundwaters of different genesis have undergone mixing, but the statistically distinct groups of $^{87}Sr/^{86}Sr$ ratios does indicate the possibility of more than one unique groundwater within the host-rock, thereby, resulting in various mineralogical reactions thus causing the discrepancy in isotopic and chemical signature shown in Figures 19 to 21.

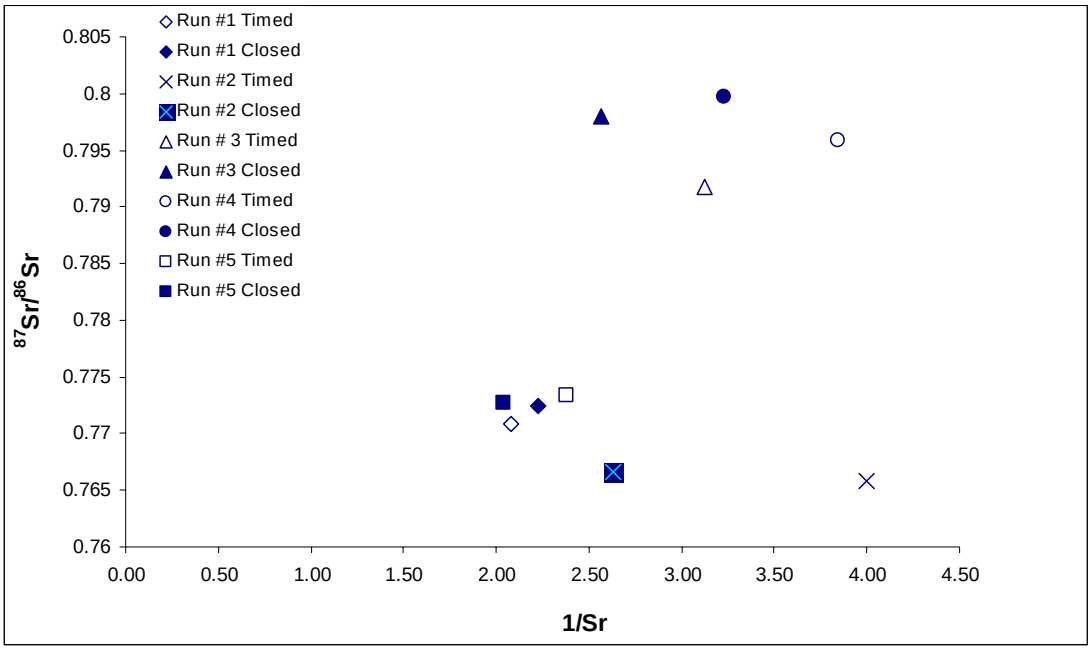

Figure 21. **$^{87}Sr/^{86}Sr$ vs. 1/Sr**

4.4 DIFFUSION MODELING

Several methods for calculating the effective diffusion coefficient were investigated in order to determine the best estimate for rates of diffusion. The rate of diffusion is essential when determining the possible travel time for radionuclide migration. Therefore, by using the effective diffusivity (De) of

a conservative ion we can estimate the rate of diffusion. Using the equation for effective diffusivity (equation 3), tortuosity (τ) (equation 4) and the molecular diffusion coefficient of free water (D_o=1.0 x10^{-9}), the effective diffusivity for diffusion experiments 1 through 5 (for the timed experiments and not the closed cells) were calculated to be 2.8 *10^{-17} m^2/s and 2.97 *10^{-17} m^2/s for the two new boreholes PFL 1 and PFL 2, respectively.

These diffusivity values demonstrate that diffusion rates are approximately equal in both boreholes (PFL-1 and –2). This is in agreement with the data shown in the breakthrough curves in Figure 7. The rate of effective diffusivity was then calculated using the molecular diffusion coefficient of a conservative ion such as Cl^- or Br whereby, Do =2.0*10^{-9}. The rates of effective diffusivity (calculated based on Fick's law) were found to be several orders of magnitude lower than those calculated by Vilks et al., (1999), 2.4*10^{-12} m^2/s and four orders of magnitude lower than in-situ values (10^{-13} m^2/s).

The discrepancy between diffusivity measurements is believed to be the result of stress release within the rock upon removal of the core, heterogeneity, and temperature.

The greater the depth at which the core is removed the greater the stress release. This would increase the potential for micro-fracturing and thereby increase the effective diffusivity measurement.

Heterogeneity of the core, specifically, variations in tortuosity also play a significant role in the rate of effective diffusivity, De. Differences in tortuosity (i.e. the flow path) are influenced by numerous factors such as porosity and grain size. In addition, temperature plays a significant role, and is proportional to the rate of diffusion. Therefore, a change in any one of these parameters can significantly influence the tortuosity factor, thus changing D_e.

4.4.1 Mathematical model for out-diffusion

In order to determine the effective diffusion coefficient a modified, three-dimensional version of the diffusion model by Van Rees, et al., (1991) was developed. The analytical solution is based on the work done by Sudicky (pers. communication, 2006) and is located in Appendix B. The model is based on two main assumptions, the first being that diffusion is one dimensional. That is, solutes are diffused out of the rock and into the reservoir and the sample is treated as semi-infinite. The second is that, diffusion is occurring radially in one dimension but remains perpendicular to the side of the core sample (i.e. $r = R_s$).

The modelled results are illustrated in Figure 22, and all five plots exhibit the same trend, whereby the breakthrough curves increase with time rather than approaching a steady-state concentration, as seen from the actual out-diffusion data. As a result, the simulated and measured results do not correlate as expected, suggesting that perhaps some of the assumptions from the analytical solution have not been met (for example, not all the pore fluids are accessible).

The analytical solution (see Appendix B) requires that an initial concentration of pore fluid salinity (Co), porosity (θ), and the volume of the reservoir (V_R) be known therefore, the initial pore fluid salinity is calculated for each of the individual diffusion experiments. An example calculation is provided in Appendix B. The Co, θ and V_R values are then input into the analytical solution to produce the simulated breakthrough curves. The modelled data however, did not provide a best fit to the actual breakthrough curves. As a result, the values for porosity and De had to be modified in order to properly curve match the results. However, a proper match could only be achieved at early time. It should be noted that, in the analytical solution (see Appendix B), porosity and De are not independent variables, (θDe,). In other words as the value of porosity is adjusted, so is the rate of effective diffusivity.

There are several explanations for why the model did not properly match to the breakthrough curves. First, the analytical solution has limitations, because it does not take into consideration any

possible chemical reactions which may have occurred during the out-diffusion experiment. For example, it does not account for precipitation reactions which may cause pore spaces to become blocked and thereby reduce the rate out-diffusion. In addition, the solution does not account for any outside damage to the core such as micro-fracturing (due to stress release upon removal of the rock core) which may increase the rate of diffusion. In other words, diffusion may have only occurred in the outer few centimetres of the core, where porosity is the greatest due to these stress releases. Therefore, the dissolved constituents of the fluid (pore fluid) located within the center of the core are inaccessible due to low porosity and permeability and hence, causes concentrations to suddenly approach a quasi steady-state.

Other limitations in the model involve the values calculated for the initial pore water concentration (Co). These initial concentrations are based on estimates of porosity and volume. Any variations between the actual porosity and volume measurements versus the calculated values will therefore, also greatly affect the rate of effective diffusivity.

Based on the best fit line (matched to early time data), the analytical solution produced effective diffusivity values that ranged between 0.244 cm^2/day (2.82 *10^{-10} m^2/s) and 0.0173 cm^2/day (2.0*10^{-11} m^2/day) for boreholes PFL-1 and -2 (see Figure 22).

These values are three to four orders of magnitude greater than those calculated using the equation $De = \theta\tau Do$ (i.e. based on measurements of θ), and hence provide a more conservative estimate for the rate of effective diffusivity. In addition, the porosity values needed to curve match to the original data were also found to be twice as large (0.0051 and 0.0058) compared to porosity values determined experimentally (0.0027). It should be noted that, the initial pore fluid concentration (Co) was not significantly modified in order to curve match the analytical solution to the original data unlike porosity and hence De (θDe), suggesting that the model supports our estimates of pore fluid salinity. This is determined based on the slope of the curve which is predominantly influenced by the value of Co. Based on our input for Co, the modelled data at early time matched almost exactly the slope (at early

time) from our experimental results. Conversely, the analytical solution required porosity and De values to be much greater than values measured experimentally. As a result, when trying to estimate the rate of effective diffusion (i.e. possible travel times for radionuclide migration) it is best to use a conservative value for rates of effective diffusion. In other words, overestimating the rate of effective diffusion would be favoured versus an underestimate of De.

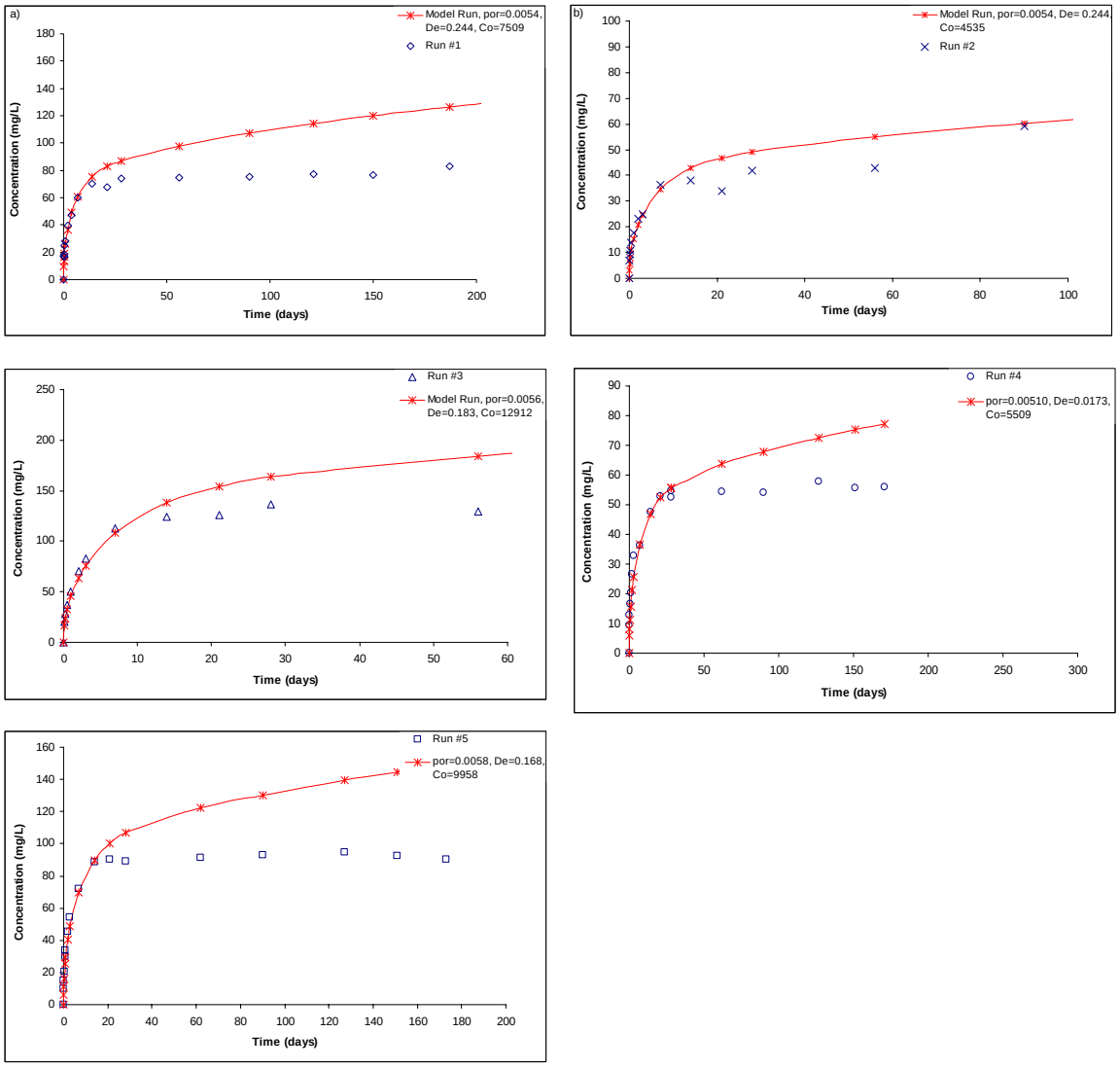

Figure 22. Breakthrough Curves for Diffusion Experiments 1 to 5

The solid line represents the modeled results, and the dotted points represent the actual data collected from the out-diffusion experiments.

CHAPTER 5. SUMMARY AND CONCLUSION

The breakthrough curves generated from each of the six, timed diffusion experiments exhibited a similar trend (with the exception of experiment #2), whereby Cl^- concentrations increased rapidly at early time, then began to plateau as steady-state concentrations were reached. The length of time required for each diffusion experiment to approach steady-state was also the same at approximately 4 weeks.

Based on the breakthrough curve data, the out-diffusion technique is a successful method for accessing pore fluid (i.e. solutes) within connected pore spaces.

Although similarities existed between each of the diffusion experiments, a major difference was measured in the chemical composition of the final solution at steady-state conditions. These differences were significant given the relative homogeneity of the core, and the relative proximity (within the wall rock) of the two boreholes to one another. Therefore, the heterogeneity of the core is assumed to be sufficient enough to alter the elemental composition of the pore fluid under water-rock interaction. The isotopic data also confirms the heterogeneity of the core as a dominant control on pore fluid chemistry.

In an attempt to explain the chemical heterogeneity observed in the diffusion experiments several different methods were employed. These methods involved crush and leach, isotope and diffusivity measurements.

The crush and leach methods found that as grain size decreased the amount of leachable Cl^- increased slightly and was independent of water-rock ratios or leach time. The results also found that fluid inclusions were not significantly impacting pore fluid salinity and hence, were not responsible for the difference in steady-state C^{l-} concentrations observed in the out-diffusion experiments.

The $\delta^{18}O$ and $\delta^{2}H$ values obtained from the diffusion experiments were found to plot above and to the left of the GMWL, which has been found to be a unique characteristic of shield brines. However,

by using such isotopically negative water as the original reservoir solution (δ^2H= -1000‰ in experiments #4 and 5), we were unable to estimate the original isotopic composition of the pore fluid, because the reservoir masked the true isotopic signature of the pore fluid.

Isotopic data obtained from seepage waters within open boreholes at the URL suggest the isotopic signature of pore fluid should vary between -8.0 and -16.0‰ for ^{18}O and -14.0 to -40.0‰ for ^2H. As a result, future work should include the use of a water source with a negative ^2H signature greater than -40‰ but not as large as -917‰.

The analytical results obtained from the ^{37}Cl measurements had a positive correlation with Cl^- concentrations suggesting a single groundwater source, with no evidence of a second end-member, however the $^{87}Sr/^{86}Sr$ results were not in accordance with these findings.

Three isotopically unique fingerprints were measured from the final solutions obtained from the out-diffusion experiments, suggesting either 1) groundwater equilibrium with the various mineral phase(s), or 2) the existence of more than one groundwater within close proximity to one another. Nonetheless, the ^{37}Cl data suggest the latter is not a realistic scenario.

The enriched ^{37}Cl values are attributed to the biotite content in the rock core, and suggest that small heterogeneities in the bulk mineral composition can generate statistically unique isotopic compositions in the pore fluid signatures, particularly in rocks which have undergone long-term equilibrium with the dominant mineral phase(s).

Strontium ratios were also significantly enriched (0.765 to 0.799) relative to $^{87}Sr/^{86}Sr$ ratios previously obtained in groundwater studies from the Lac du Bonnet Batholith (0.714-0.735). The $^{87}Sr/^{86}Sr$ ratios suggest equilibrium with minerals rich in Rb, poor in Sr concentration. Although the ^{87}Sr signature is much larger in minerals such as muscovite and K-feldspar their dissolution rates are several orders of magnitude greater than less Rb rich minerals such as plagioclase. Therefore, mica and K-feldspar would have had to be in abundance and in long-term equilibrium with the groundwater in order

to cause a shift in the isotopic composition of the pore fluids. Whole-rock analyses confirmed that biotite was not the dominant mineral phase in either borehole (PFL -1 and -2). Therefore, Sr isotopic signatures were most likely derived from long-term exchange reactions between pore fluid and K-feldspar. The research conducted by McLaughlin, (1997) also found pore fluid signatures to be representative of K-feldspar dissolution. In addition, ^{87}Sr signatures obtained by McLaughlin (1997), were also enriched and were within the same range as those obtained from the out-diffusion experiments.

Future research should include the isotopic analyses of individual mineral phases as another means of confirming the extent/influence of water-rock interaction.

The rates of effective diffusivity were calculated for each timed, out-diffusion experiment using two different methods. The purpose for calculating De was to establish whether or not the cores exhibited a difference in the rate of diffusion which may be contributing to the difference in Cl^- concentration observed between experiments 1 through 5. The first method involved an estimated tortuosity factor. The second method involved the use of a three- dimensional diffusivity model.

The De values calculated using the analytical model were three to four orders of magnitude greater (10^{-10} and 10^{-11} m^2/s) than those determined experimentally using the equation $De = \theta\tau Do$ (10^{-17} m^2/s). In addition, the model did not approach steady-state conditions as did the experimental results. Therefore, curve matching the model to the laboratory results was only successful at early time and required porosity values to be modified. As a result, porosity values based on the analytical solution were two times greater than those calculated experimentally. Therefore, the rate of diffusivity can be determined using an analytical solution however, the model has limitations and the value of De should be used as a conservative estimate only.

In summary, the out-diffusion experiment was a viable method for matrix pore fluid (i.e. solute) extraction, and given an appropriate core size and reservoir volume, the experiments were able to achieve steady-state conditions in as little as one month.

Chemical and isotopic analyses such as, Cl^-, ^{37}Cl, ^{18}O, ^{2}H and ^{87}Sr were also shown to be valuable in characterizing the signature of the pore fluids and in helping to identify the original pore fluid source(s). Isotope analyses such as, ^{18}O and ^{2}H can be valuable for assessing the origin and evolution of pore fluids however, during this study ^{18}O and ^{2}H were not successful due to the highly negative isotopic signature of the reservoir water, and the small volume of pore fluid constituents extracted from the core in comparison to the reservoir volume. Therefore, future experiments should use a reservoir water with an isotopically deplete signature, but not so negative that it masks the signature of the original pore fluid.

Estimates of the rate of effective diffusivity (De) could be evaluated based on the experimental breakthrough curves and/or by a modified three-dimensional analytical solution. A comparison of both methods found a large discrepancy between the values, which was likely attributed to the assumptions of the analytical solution (i.e. assumes complete pore fluid extraction). Therefore, the design of future out-diffusion experiments should reduce and/or minimize these assumptions (i.e. restrict, if possible, out-diffusion from the top and bottom of the core segments).

REFERENCES

Arjang, B. and G. Herget, 1997. In situ ground stresses in the Canadian hardrock mines: An update. International Journal of Rock Mechanics and Mineral Science, **34**, 3-4, pp.16

Becker, M.W. and A.M. Shapiro, 2000. Tracer transport in fractured rock: Evidence of non-diffusive breakthrough tailing. Water Resour. Res, **36**, 1677-1686.

Boving, T.B. and P. Grathwohl, 2001. Tracer diffusion coefficients in sedimentary rocks: correlation to porosity and hydraulic conductivity. Journal of Contaminant Hydrology, **53**, 85-100.

Blyth, A., 2004. Radioactive Waste Disposal in the crystalline rock of Scandinavia: case studies of the far-field environment. Unpublished Ph.D. Thesis, University of Waterloo, Waterloo, Ontario, Canada.

Brown, A., C.D. Kamineni and D. Martin, 1990. In situ stress compared to structures in Lac du Bonnet Batholith Manitoba, Canada. Tectonphysics, **186**, 151-162.

Clauer, N., S.K. Frape. and B. Fritz, 1989. Calcite veins of the Stripa granite (Sweden) as records of the origin of the groundwaters and their interactions wit the granitic body. Geochimica et Cosmochimica Acta, **53**, 1771-1781.

Couture, R.A., M.G. Seitz and M.J. Steindler, 1983. Sampling of brine in cores of Precambrian granite from northern Illinois. Journal of Geophysical Research, **88**, 7331-7334.

Craig, H., 1961a. Isotopic Variations in meteoric waters. Science, **133**, 1702-1703.

Craig, H., 1961b. Standard for reporting concentrations of deuterium and oxygen-18 in natural waters. Science, **133**, 1833-1834.

Davison, C.C., 1984. Monitoring hydrogeological conditions in fractured rock at the site of Canada's Underground Research Laboratory: Monitoring Groundwater, **4**, 95-102.

Eastoe, C.J., J.M. Guilbert and R.S. Kaufmann, 1989. Geology, **17**, pp285

Epstein, S. and T. Mayeda, 1953. Variation of ^{18}O content of waters from natural sources. Geochimica et Cosmochimica Acta, 4, 213-224.

Ercho, G., 1998. A profile of leachable ions in a major fracture zone. AECL, Applied Geoscience Branch, Pinawa, Manitoba, Canada, 13p.

Fairhurst, C., 2004. Nuclear waste disposal and rock mechanics: contributions of the Underground Research Laboratory (URL), Pinawa, Manitoba, Canada. International Journal of Rock Mechanics and Mining Sciences, **41**, 1221-1227.

Fetter, C.W., 2001. Applied Hydrogeology. Prentice-Hall, Inc., New Jersey, 400-402.

Franklyn, M.T., R.H. McNutt, D.C. Kamineni, M. Gascoyne, and S.K. Frape, 1991. Groundwater $^{87}Sr/^{86}Sr$ values I the Eye-Dashwa Lakes pluton, Canada: Evidence for plagioclase-water reaction. Chemical Geology, **86**, 111-122.

Frape, S.K. and P. Fritz, 1984. Water-rock interaction and chemistry of groundwaters from the Canadian Shield. Geochimica et Cosmochimica Acta, **48**, 1617-1627.

Frape, S.K. and P. Fritz, 1987. Geochemical Trends for Groundwaters from the Canadian Shield. Geological Association of Canada Special Paper **33**. pp. 19-38.

Frape, S.K., A. Blyth, R. Blomqvist, R.H. McNutt and M. Gascoyne, 2004. Deep fluids in the continents: II. Crystalline rocks, pp. 541-579. In Surface and Ground Water, Weathering, and Soils (ed. J.I. Drever) Vol. 5 Treatise on Geochemistry (eds. H.D. Holland and K.K. Turekian), Elsevier-Pergamon, Oxford.

Freeze, R.A. and J.A. Cherry, 1979. Groundwater. Prentice-Hall, Inc., New Jersey, 103-105.

Fritz, P. and S.K. Frape, 1982. Saline groundwaters in the Canadian Shield- A first overview. Chemical Geology, **36**, 179-190.

Fritz, B., N. Clauer and M. Kam, 1987. Strontium isotopic data and geochemical calculations as indicators for the origin of saline waters in crystalline rocks. Geological Association of Canada Special Paper **33**, 121-126.

Gascoyne, M., C.C. Davison, J.D. Ross, and R. Pearson, 1987. Saline Groundwaters and Brines in Plutons in the Canadian Shield. Saline Water and Gases in Crystalline Rocks, pp. 53-68.

Gascoyne, M., J.D. Ross, R.L. Watson and D.C. Kamineni, 1989. Soluble salts in a Canadian Shield granite as contributors to groundwater salinity. Water-Rock Interaction, 247-249.

Gascoyne, M. and D.C. Kamineni, 1994. The hydrogeochemistry of fractured plutonic rocks in the Canadian Shield. Applied Hydrogeology, **2**, 43-49.

Gascoyne, M., 2004a. Determination of matrix pore fluid composition and application to site characterization. Gascoyne GeoProjects Inc. pp.18.

Gascoyne, M., 2004b. Hydrogeochemistry, groundwater ages and sources of salts in a granitic batholith on the Canadian Shield, southeastern Manitoba. Applied Geochemistry. **19**, 4, 519-575.

Gascoyne, M., J. McMurray and R. Ejeckam, 2004. Paleohydrogeologic case study of the Whiteshell research area. OPG, report no. 06819-REP-01200-10121-R00, Toronto, Ontario, Canada, 118p.

Goldich, S.S., 1938. A study in rock weathering. Journal of Geology, **46**, 17-58.

Haimson, B., M. Lee, N. Chandler and D. Martin, 1993. Estimating the state of stress from subhorizontal hydraulic fractures at the Underground Research Laboratory, Manitoba. International Journal of Rock Mechanics, Mineral Science and Geochemical Abstracts, **30**, 7, 959-964.

Hoering T.C. and P.L. Parker, 1961. Geochimica et Cosmochimica Acta, **23**, pp185

Kloppman, W., J.P. Girard and P. Négrel, 2002. Exotic stable isotope compositions of saline waters and brines from the crystalline basement. Chemical Geology, **184**, 49-70.

Larson, S.A. and E-L. Tullborg, 1983. Stable isotope evidence on the origin of calcite fissure fillings within the Svecokarelian province of Sweden In: Proceedings of the 4th International Symposium on Water-Rock Interaction (WRI-4), 265-268.

Le Glovan, Y.M., J.L. Michelot and J.Y. Boisson, 1997. Stable isotope contents of porewater in a claystone formation (Tournemire, France): assessment of the extraction technique and preliminary results. Applied Geochemistry, **12**, 739-745.

Li, W., M.T. Franklyn, R.H. McNutt, H.P. Schwarcz,, M. Gascoyne, D.C. Kamineni and S.K. Frape, 1989. A Sr isotopic study of the Eye-Dashwa Lakes pluton, Ontario and the Lac du Bonnet pluton, Manitoba: Plagioclase/water reaction. Water-Rock Interaction, 441-444.

Lindblom, S., A. Blyth, S. Gehor, N. Waber and S. Frape, 2002. Matrix fluid chemistry experiment: Quartz-fluid interaction-fluid inclusions and the matrix fluid. Synthesis of an inter-laboratory study, Djupforvarsteknik. SKB TD-03-02, Svensk Karnbranslehantering AB.

Liu, H.H., G.S. Bodvarsson and G. Zhang. Scale dependency of the effective matrix diffusion coefficient. Vadose Zone Journal, **3**, 312-315.

Martin, C.D. and N.A. Chandler, 1993. Stress Heterogeneity and Geological Structures. International Journal of Rock Mechanics, Mineral Science and Geochemical Abstracts, **30**, 7, 993-999.

McNutt, R.H., S.K. Frape and P. Fritz, 1984. Strontium isotopic composition of some brines from the Precambrian Shield of Canada. Isotope Geoscience, 205-215.

McNutt, R.H., 1987. 87Sr/86Sr Ratios as Indicators of Water/Rock Interactions: Application to brines found in precambrian age rocks from Canada. Geological Association of Canada Special Paper **33**, 81-88.

McNutt, R.H., S.K. Frape, P. Fritz, M.G. Jones and I.M. MacDonald, 1990. The 87Sr/86Sr values of Canadian Shield brines and fracture minerals with applications to groundwater mixing, fracture history, and geochronology. Geochemica et Cosmochimica Acta, **54**, 205-215.

McNutt, R.H., 2000. Strontium isotopes. Environmental Tracers in Subsurface Hydrology (eds. Cook, P. and Herczeg, A.L.), Kluwer Academic Publishers, 234-260.

Melynk, T.W. and M.M. Skeet, 1986. An improved technique for the determination of rock porosity. Can. J. Earth Sci., **23**, 1068-1074.

Moreau-Le Golvan, Y., J.L. Michelot and J.Y. Boisson, 1997. Stable isotope contents of porewater in a claystone formation (Tournemire, France): assessment of the extraction technique and preliminary results.

Morrison, J., T. Brockwell, T. Merren, F. Fourel and A.M. Phillips, 2001. On-line high precision stable hydrogen isotopic analyses on nanoliter water samples. Analytical Chemistry, **73**, 3570-3575.

Nesbitt, H.W., 1985. A chemical equilibrium model for the Illinois basin formation waters. American Journal of Science, **285**, 436-458.

Négrel, P., J. Casanova and J.F. Aranyossy, 2001. Strontium isotope systematics used to decipher the origin of groundwaters sampled from ganitoids: the Vienne case (France). Chemical Geology, **177**, 287-308.

Négrel, P., J. Casanova and R. Blomqvist, 2005. $^{87}Sr/^{86}Sr$ of brines from the Fennoscandian Shield: a synthesis of groundwater isotopic data from the Baltic Sea region. Canadian Journal of Earth Science., **42**, 273-285.

Nordstrom, D.K., J.W. Ball, R.J. Donahoe and D. Whittemore, 1989a. Groundwater chemistry and water-rock interactions at Stripa. Geochimica et Cosmochimica Acta, **53**, 1723-1740.

Nordstrom, D.K., S. Lindblom, R.J. Donahoe and C.C. Barton, 1989b. Fluid inclusions in the Stripa granite and their possible influence on the groundwater chemistry. Geochimica et Cosmochimica Acta, **55**, 1741-1765

Rasilainen, K., K.H. Hellmuth, L. Kivekäs, A. Melamed, T. Ruskeeniemi, M.S. Kauppi, J. Timonen and M. Valkiaien, 1996. An interlaboratory comparison of methods for measuring rock matrix porosity. VTT, Julkaisija-Utgivare Publishing, 15p.

Roedder, E., 1984. Fluid inclusions. Mineralogical Society of America, Reviews in Mineralogy, 12, 646p.

Ropchan, J.C., 1997. Evidence of Stable chlorine isotope fractionation in selected silicate minerals due to crystal structure and formational histories using different Cl extraction techniques. B.Sc. thesis, Earth Sciences, University of Waterloo, 74p.

Rübèl, A.P., C. Sonntag, J. Lippmann, F.J. Pearson and A. Gautschi, 2002. Solute transport in formations of very low permeability: Profiles of stable isotope and dissolved nobel gas contents of pore water in the Opalinus Clay, Mont Terri, Switzerland. Geochimica et Cosmochimica Acta, **66**, 8, 1311-1321.

Savoye, S., J.F. Aranyossy, C. Beaucaire, M. Cathelineau, D. Lovat and J.L. Michelot, 1998. Fluid inclusions in granite and their relationships with present day groundwater chemistry. European Journal of Mineralogy, **10**, 1215-1226.

Shouakar-Stash, O., R.J. Drimmie and S.K. Frape, 2005. Determination of inorganic chlorine stable isotopes by continuous flow isotope ratio mass spectrometry. Rapid Commun. Mass Spectrom, **19**, 121-127.

Shouakar-Stash, O., S.V. Alexeev, S.K. Frape, L.P. Alexeeva and R.J. Drimmie, 2007. Geochemistry and stable isotopic signatures, including chlorine and bromine isotopes, of the deep groundwaters of the Siberian Platform, Russia. Applied Geochemistry, **22**, 589-605.

Sie, P.M.J. and S.K. Frape, 2002. Evaluation of the groundwaters from the Stripa mine using stable chlorine isotopes. Chemical Geology, **182**, 565-582.

Skoog, D.A. and D.M. West, 1982. Fundamentals of analytical chemistry. Saunders College Publishing, 40-91.

Stevenson, D.R., E.T. Kozak, C.C. Davison, M. Gascoyne and R.M. Broadfoot, 1996. Hydrogeologic characteristics of domains of sparsely fractured rock in the granitic Lac du Bonnet Batholith, Southwestern Manitoba, Canada. Atomic Energy of Canada Limited Report, AECL -11558, C06-96-17.

Stewart, M.K. and I. Friedman, 1975. Deuterium fractionation between aqueous salt solutions and water vapour. Journal of Geophysical Research. **88**, 27, 3812-3818.

Stewart, M.A. and A.J. Spivack, 2004. The stable-chlorine isotope compositions of natural and anthropogenic materials. Reviews in Mineralogy and Geochemistry, **55,** 231-254.

Tullborg, E.L., 2001. Matrix pore fluid chemistry experiment, porosity and density measurements on samples from drillcore KF0051A01. SKB. International Technical Document ITD-01-03, 23p.

Tyedmers, P.H., 1987. Leachable chloride in the Lac du Bonnet Batholith granite. AECL, Applied Geoscience Branch, Pinawa, Manitoba, Canada. 18p.

Van Rees, K.C.J., E.A. Sudiky, S.C. Rao and K. Ramesh Reddy, 1991. Evaluation of Laboratory Techniques for Measuring Diffusion Coefficients in Sediments. Environmental Science and Technology, **25**, 1605-1611.

Vilks, P., J.J. Cramer, T.W. Melynk, F.W. Stanchell, N.H. Miller and H.G. Miller, 1999. In-situ diffusion in granite: phase I final report. OPG, Nuclear Waste Management, report no.06819-REP-01200-0087-R00, Toronto, Ontario, Canada, 107p.

Vilks, P., N.H. Miller and F.W. Stanchell, 2004. Phase II in-situ diffusion experiment. OPG, Nuclear Waste Management, report no. 06819-REP-01200-10128-R00, Toronto, Ontario, Canada, 199p.

Waber, N. and J. Smellie, 2004. Oskarshamn site investigation borehole KSH02: Characterisation of matrix pore water (feasibility study). SKB International Technical Document P-04-249, 54p.

Waber, N. and S.K. Frape, 2002. Matrix fluid chemistry experiment, synthesis report: drillcore pore water leaching studies and borehole water. SKB technical report, TD-03-02, 67p.

APPENDIX A

Table A1

Diffusion Run	Time (days)	Extracted Sample Weight (g)	Dilution Weight (g)	Weight of Ultrapure Water Added (g)	Cl Concentration as Reported by the Lab (mg/L)	Calculated Cl Concentration (mg/L)
PFL 2-34 First Run	0.0125	NA	NA	NA	18.3	18.3
	0.25	0.32	5.00	4.68	1.1	17.19
	0.375	0.49	5.00	4.51	1.6	16.33
	0.5	0.4	4.99	4.59	1.5	18.38
	1	0.34	5.01	4.67	1.7	25.05
	2	0.36	5.05	4.69	2.0	28.06
	4	0.38	5.07	4.69	2.96	39.49
	7	0.34	5.00	4.66	3.23	47.5
	14	0.34	5.13	4.79	3.96	59.75
	21	0.34	5.00	4.66	4.81	70.22
	28	0.62	4.99	4.37	8.37	67.37
	56	0.35	5.00	4.65	5.2	74.29
	90	0.37	3.01	2.64	9.22	74.84
	121	0.37	3.04	2.67	9.23	75.59
	150	0.39	3.01	2.62	10	77.18
	187	0.48	2.99	2.51	12.3	76.62
	211	0.34	2.99	2.65	9.47	83.28
	239	0.40	3.01	2.61	10.5	75.25
PFL 2-13 Second Run	0.04	0.38	5.10	4.72	0.52	6.98
	0.13	0.36	5.00	4.72	0.52	6.98
	0.25	0.38	5.35	4.97	0.76	10.70
	0.50	0.31	5.45	5.14	0.79	13.89
	1	0.39	5.02	4.63	1.38	17.76
	2	0.39	2.99	2.60	3.03	23.23
	3	0.34	3.00	2.66	2.82	24.88
	7	0.31	3.00	2.69	3.74	36.19
	14	0.36	2.99	2.63	4.57	37.96
	21	0.36	3.00	2.64	4.05	33.75
	28	0.33	3.02	2.69	4.56	41.73
	56	0.32	3.01	2.69	4.55	42.80
	90	0.36	2.97	2.61	7.13	59.22
	120	0.30	3.00	2.7	6.72	67.20
	150	0.38	3.07	2.69	5.52	44.60
	181	0.38	3.16	2.78	5.16	42.91
	231	0.31	3.01	2.70	5.34	51.85
	240	0.34	3.00	2.66	6.01	53.03
	247	0.32	3.00	2.68	5.65	52.97

Diffusion Run	Time (days)	Extracted Sample Weight (g)	Dilution Weight (g)	Weight of Ultrapure Water Added (g)	Cl Concentration as Reported by the Lab (mg/L)	Calculated Cl Concentration (mg/L)
PFL 1-14 Third Run	0.125	0.33	5.04	4.71	1.32	20.16
	0.25	0.36	4.97	4.61	2.02	27.89
	0.5	0.38	4.96	4.58	2.8	36.55
	1	0.36	4.98	4.62	3.61	49.94
	2	0.36	3.00	2.64	8.48	70.67
	3	0.38	2.98	2.60	10.6	83.13
	7	0.36	3.00	2.64	13.5	112.50
	14	0.36	2.99	2.63	14.9	123.75
	21	0.35	3.02	2.67	14.6	125.98
	28	0.36	3.03	2.67	16.19	136.27
	56	0.37	3.09	2.72	15.46	129.11
	90	0.39	3.01	2.62	17.1	131.98
	120	0.35	3.00	2.65	15.3	131.14
	150	0.33	2.96	2.63	15.6	140.40
	181	0.38	3.01	2.63	17.6	139.41
	201	75	0	0	130.00	130.00
PFL 1-19 Fourth Run	0.04	0.39	3.00	2.61	1.22	9.38
	0.13	0.38	3.00	2.62	1.63	12.87
	0.25	0.36	3.00	2.64	1.98	16.50
	0.50	0.37	3.01	2.64	2.49	20.26
	1	0.33	2.99	2.66	2.92	26.46
	2	0.30	2.99	2.69	3.29	32.79
	3	0.35	3.01	2.66	4.23	36.38
	7	0.36	3.03	2.67	5.63	47.39
	14	0.33	2.99	2.66	5.84	52.91
	21	0.33	2.99	2.66	6.03	54.64
	28	0.34	2.99	2.65	5.96	52.41
	62	0.39	2.99	2.60	7.1	54.43
	90	0.37	2.99	2.62	6.7	54.14
	127	0.36	2.98	2.62	6.98	57.78
	151	0.38	3.12	2.74	6.77	55.59
	171	75	0	0	56.00	56.00
PFL 2-19 Fifth Run	0.04	0.39	3.00	2.61	1.3	10.00
	0.13	0.41	2.98	2.57	2.03	14.75
	0.29	0.32	3.00	2.68	2.2	20.63
	0.75	0.34	3.00	2.66	3.29	30.00
	1	0.36	3.01	2.65	4.02	33.61
	2	0.37	2.00	1.63	5.59	45.32
	3	0.35	3.01	2.66	6.29	54.09
	7	0.31	3.00	2.69	7.44	72.00
	14	0.36	3.00	2.64	10.6	88.33
	21	0.33	3.04	2.71	9.78	90.09
	28	0.33	2.99	2.66	9.81	88.88
	62	0.35	3.05	2.70	10.5	91.5

Diffusion Run	Time (days)	Extracted Sample Weight (g)	Dilution Weight (g)	Weight of Ultrapure Water Added (g)	Cl Concentration as Reported by the Lab (mg/L)	Calculated Cl Concentration (mg/L)
	90	0.37	3.00	2.63	11.5	93.24
	127	0.32	2.99	2.67	10.13	94.65
	151	0.33	3.00	2.67	10.16	92.36
	173	75	0	0	90.00	90.00
PFL 2-25 Oxygen-Free	0.04	0.34	3.00	2.66	0.98	8.65
	0.13	0.45	3.01	2.56	1.81	12.11
	0.25	0.40	3.01	2.61	2.23	16.78
	0.38	0.33	3.06	2.73	1.91	17.71
	1	0.38	3.01	2.63	3.67	29.07
	1.88	0.32	3.00	2.68	3.71	34.78
	2	0.32	3.02	2.70	3.81	35.96
	3	0.30	3.00	2.70	4.28	42.80
	6	0.30	3.00	2.70	5.63	56.30
	14	0.30	3.00	2.70	5.74	57.40
	21	0.30	3.00	2.70	5.82	58.2
	86	75	0	0	55	55
PFL 2-34 Repeat	0.04	0.39	3.03	2.64	1.71	13.29
	.17	0.47	3.02	2.55	0.30	1.93
	0.25	0.30	2.99	2.69	0.36	3.59
	0.42	0.34	3.03	2.69	.17	1.52
	0.88	0.34	3.09	2.75	0.24	2.18
	1	0.38	3.00	2.62	0.19	1.50
	1.96	0.26	2.95	2.69	0.21	2.38
	3	0.32	3.00	2.68	0.26	2.44
	4.08	0.30	3.01	2.71	0.25	2.51
	7	0.31	3.01	2.70	0.28	2.72
	14	0.32	3.01	2.69	0.33	3.10
	22.13	0.31	3.00	2.69	0.25	2.42
	84	75	0	0	3.00	3.00

Table A2

Borehole ID	Sieve Size/Mesh Size (µm)	Water: Rock	Time (min)	Cl Concentration (mg/L)
Test Run	80/180	2:1	20	60.8
			40	49
			60	49.6
			80	51.2
			100	56.8
	140/106	1:1	20	NA
			40	72.1
			60	64.6
			80	69
			100	NA
	170/90	2:1	20	60.6
			40	62.8
			60	61.6
			80	65
			100	66.4
	200/75	2:1	20	57.8
			40	57
			60	55.4
			80	54.6
			100	57
	230/63	2:1	20	55.4
			40	61.6
			60	59.4
			80	59.8
			100	64.2
	450/<38	2:1	20	64.2
			40	67.8
			60	68.4
			80	73.2
			100	87.8
PFL 2-33	140/106	1:1	10	47.9
			20	48.3
			40	48.8
			60	48.5
			360	50.9
			1440	51.9
			2880	54.8
	200/75	2:1	10	49.96
			20	50.40
			45	51.26
			80	51.43
			1440	54.02
			7200	54.11

Borehole ID	Sieve Size/Mesh Size (µm)	Water: Rock	Time (min)	Cl Concentration (mg/L)
	400/38	2:1	20	60.81
			40	60.87
			80	60.88
			1200	62.65
			1440	63.46
			2880	62.27
			7200	63.01
PFL 2-14	140/106	1:1	10	27.0
			20	27.4
			40	28.4
			60	28.1
			1440	29.8
			2880	31.4
	400/38	2:1	10	58
			20	58.2
			40	59.6
			60	59
			1500	61.2
			2880	63.2

Table A3

	Sieve Size/Mesh Size (μm)	Water: Rock ratio	Cl Concentration (mg/L)
PFL 2-14	>60/>250	1:1	12.04
	80/180	2:1	12.36
	200/75	2:1	18.96
	270/53	2:1	28.96
	>400/>38	2:1	97.96
PFL 2-33	>60/>250	1:1	14.57
	80/180	2:1	15.12
	140/106	1:1	52.8
	270/53	2:1	49.72
	>400/>38	2:1	76.14

Table A4

Borehole	Leach No.	Water: Rock Ratio	Cl concentration (mg/L)
PFL 2-13	Leach #1 (Coarse Grained)	1:1	7.42
	Leach #2 (Medium Grained)	1:1	6.09
	Leach #3 (Fine Grained)	1:1	19.24
PFL 2-15	Leach #1 (Coarse Grained)	1:1	4.36
	Leach #2 (Medium Grained)	1:1	7.02
	Leach #3 (Fine Grained)	1:1	10.95
PFL 2-34	Leach #1 (Coarse Grained)	1:1	5.31
	Leach #2 (Medium Grained)	1:1	6.71
	Leach #3 (Fine Grained)	1:1	13.38

Example estimating the original δ18O and δ^2H signatures

$\delta^{18}O$ in the bulk solution (original water added to the cell)	=	-113.4‰
$\delta^{18}O$ in the final solution (after steady state was achieved)	=	-118.94‰
Taking the weight of the rock core	=	1065.65 g
Porosity	=	0.00267
Weight of water added to the cell	=	300.35 g
n_{pore})	=	?
$\delta^{18}O_{pore}$	=	?

Note: np is the fraction of pore fluid that can be extracted from rock, based on rock weight and density vs. total weight of water added to the cell.
Nb is the total fraction of bulk solution added to the cell vs. the total weight of pore fluid + bulk solution.

We want to determine the original pre water isotopic composition, therefore:

$$\delta^{18}O_{final} = n_{bulk}\delta^{18}O_{bulk} + n_{pore}\delta^{18}O_{pore}$$

$$1065.65g \times 0.00267 = 2.85g$$

$$n_{bulk} = \frac{300.35g}{300.35g + 2.85g} = \frac{300.35g}{303.19g} = 0.9906$$

$$n_{pore} = \frac{2.85g}{300.35g} = 0.00939$$

$$-118.94 = 0.99006(-113.4) + (0.00939)\delta^{18}O_{pore}$$
$$-118.94 = -112.33 + (0.00939)\delta^{18}O_{pore}$$
$$-6.61 = (0.00939)\delta^{18}O_{pore}$$
$$-703.94 = \delta^{18}O\text{pore water}$$

$$\delta^2H_{final} = n_{bulk}\delta^2H\text{bulk} + n_{pore}\delta^2H_{pore}$$

δ^2H_{final} = - 896.12‰
δ^2H_{bulk} = -917.51 ‰

$$-896.12 = 0.9906\ (-917.51) + 0.00939\delta^2H_{pore}$$
$$-896.12 = -908.88\ (-917.51) + 0.00939\delta^2H_{pore}$$
$$12.76 = 0.00939\ \delta^2H_{pore}$$
$$1358.89\ ‰ = \delta^2H_{pore}$$

Sample Calculation for Pore Fluid Salinity:

θ=0.003
r =3.05 cm
h =15 cm

$$V = \pi r^2 h$$
$$V = \pi(3.05)^2(15)$$
$$V = 438.36 cm^3$$

Where, V is the volume of the rock core, r is the radius and h is the height in cm,

m =1128.80 g (dry weight of core)
v = 438.36 cm^3

$$d = \frac{m}{v}$$

$$d = \frac{1128.80g}{438.36cm^3}$$

$$d = 2.57\frac{g}{cm^3}$$

Whereby, d is the density, m is the mass and v is the volume of the rock core, therefore, if:
Cl concentration (at steady-state) 77.78 mg/Kg

1L =1000 cm^3

$$2.57\frac{g}{cm^3} \times \frac{1000}{1}\frac{cm^3}{L} = 2570\frac{g}{L} = 2.57\frac{Kg}{L}$$

$$C \times d = \frac{mg}{L} \text{ (mg of Cl per L of rock)}$$

$$77.78\frac{mg}{Kg} \times 2.57\frac{Kg}{L} = 199.89\frac{mg}{L}\frac{ofCl}{ofRock}$$

$$\frac{1L}{x} = \frac{0.003}{1}$$
$$x = 367.64$$

$$199.89\frac{mg}{L} \times 367.64 = 73488.94\frac{mg}{L} = 73.48\frac{g}{L} \text{ of Cl per L of rock}$$

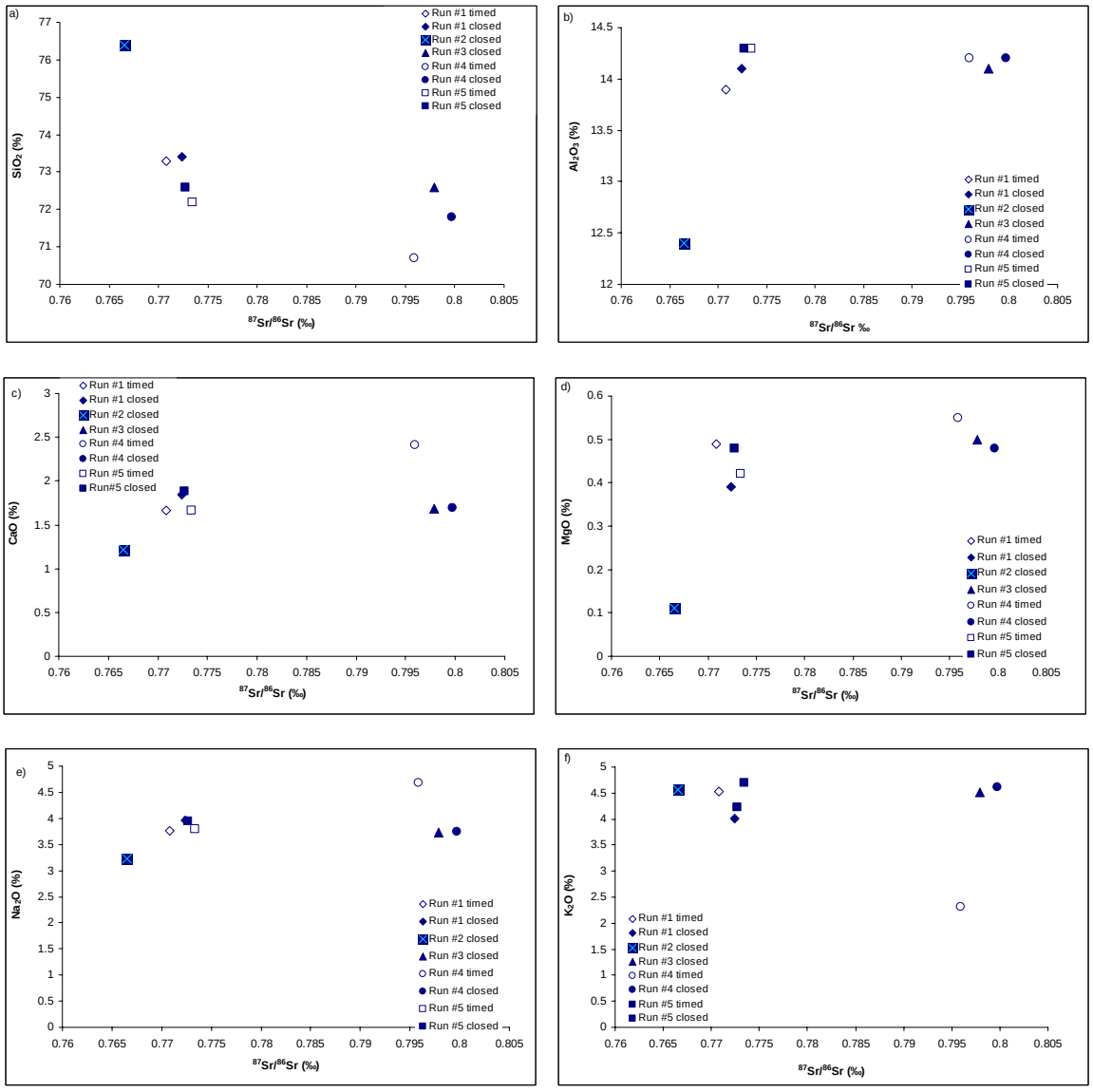
a)
SiO2 (%)
87Sr/86Sr (‰)
b)
Al2O3 (%)
87Sr/86Sr ‰
c)
CaO (%)
87Sr/86Sr (‰)
d)
MgO (%)
87Sr/86Sr (‰)
e)
Na2O (%)
87Sr/86Sr (‰)
f)
K2O (%)
87Sr/86Sr (‰)
Run #1 timed
Run #1 closed
Run #2 closed
Run #3 closed
Run #4 timed
Run #4 closed
Run #5 timed
Run #5 closed
Run#5 closed

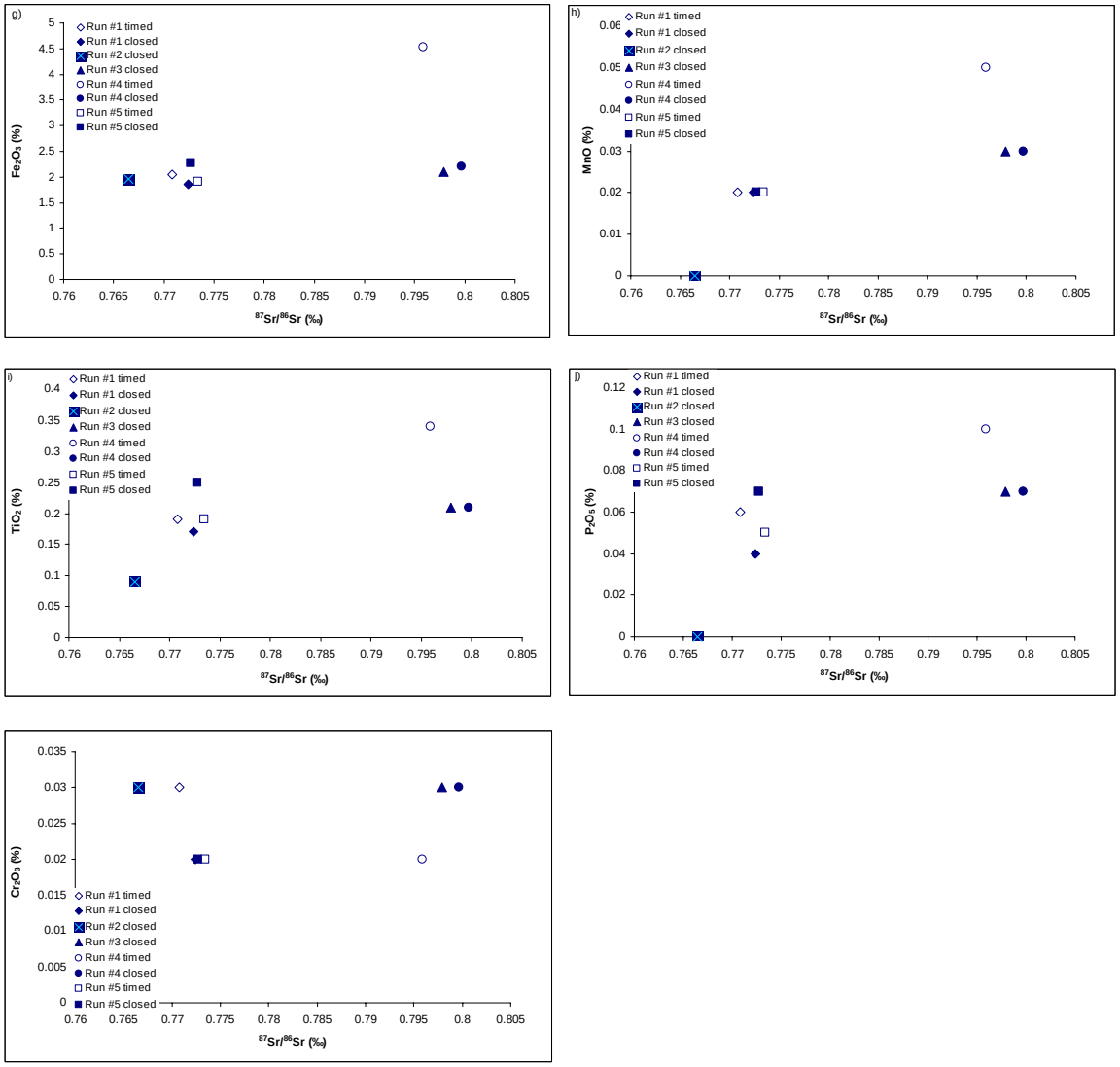

Figure A1. Graphical Representation of the Whole-rock Data

Note the positive trend in figures d, h, i and j and the decreasing trend observed in Figure a. The solid line represents the modeled results, and the dotted points represent the actual data collected from the out-diffusion experiments.

APPENDIX B

Continuity equation for the Reservoir:

$$V_R \frac{\partial C_R}{\partial t} = 2\pi {R_s}^2 \theta De \frac{\partial C_s}{\partial x}\Big|_{x=0} - 2\pi R_s L_s \theta De \frac{\partial C_s}{\partial r}\Big|_{r=Rs} \tag{B1}$$

with initial condition:

$$C_r(t=0) = 0 \tag{B2}$$

In equation (B1) we will need to include the gradients, which are obtained using the solution to Fick's second law.

$$\frac{\partial C_s}{\partial x}\Big|_{x=o} and \frac{\partial C_s}{\partial r}\Big|_{r=Rs}$$

We now need to consider diffusion from the top and bottom of the core, therefore:

$$\theta \frac{\partial C_s}{\partial t} - \theta D_e \frac{\partial^2 C_s}{\partial x^2} = 0 \text{ , } 0 \leq x \leq \infty \tag{B3}$$

$$C_s(x,0) = C_o \tag{B4a}$$

$$C_s(0,t) = Cr(t) \tag{B4b}$$

$$C_s(\infty,t) = 0 \tag{B4c}$$

Next, the Laplace transform equation $\left(C_s(x,p) = \int_0^\infty C_s(x,t)\exp(-pt)dt \right)$ is transformed and applied to equation (B3) and (B4) to get:

$$\frac{d^2\overline{C}}{dx^2} - \frac{P}{De}\overline{C} = -\frac{C_o}{De} \tag{B5}$$

Subject to:

$$C_s(0,p) = \overline{C}_R(p) \tag{B6a}$$

$$C_s(\infty,p) = 0 \tag{B6b}$$

Thus, the general solution to equation B5 is:

$$C_s = A\exp\left\{-\left(\frac{P}{De}\right)^{1/2}x\right\} + B\exp\left\{\left(\frac{p}{De}\right)^{1/2}x\right\} + \frac{C_o}{p} \tag{B7}$$

The boundary condition, defined by equation (B6b) requires that B=0, and using equation (B6a) we obtain:

$$\overline{C}_R = A + \frac{C_o}{P} \text{ , or}$$

$$\overline{C}_s = \overline{C}_R - \frac{C_o}{P} \tag{B8}$$

Hence, we now have:

$$\overline{C}_s = \left(\overline{C}_R - \frac{C_o}{P}\right)\exp\left\{-\left(\frac{P}{De}\right)^{1/2}\right\} + \frac{C_o}{P} \tag{B9}$$

We will later need the Laplace transform of the gradient at x=0, it is from equation (B9):

$$\frac{d\overline{C}_s}{dx}\Big|_{x=0} = -\left(\frac{P}{De}\right)^{1/2}\left[\overline{C}_R - \frac{C_o}{P}\right] \tag{B10}$$

Next, we will consider the 1 dimensional radial diffusion problem. We have:

$$\theta\frac{\partial C_s}{\partial t} - \theta De\left[\frac{\partial^2 C_s}{\partial r^2} + \frac{1}{r}\frac{\partial C_s}{\partial r}\right] = 0 \quad 0 \le r \le R_s \tag{B11}$$

with,

$$C_s(r,0) = C_o \tag{B12a}$$

$$C_s(R_s,t) = C_R(t) \tag{B12b}$$

$$\frac{\partial C_s}{\partial r}(0,t) = 0 \tag{B12c}$$

Application of the Laplace transform leads to:

$$p\overline{C}_s - C_o - De\left[\frac{d^2\overline{C}_s}{dr^2} + \frac{1}{r}\frac{d\overline{C}s}{dr}\right] = 0 \text{ or}$$

$$\frac{d^2\overline{C}_s}{dr^2} + \frac{1}{r}\frac{d\overline{C}_s}{dr} - \frac{P}{De}\overline{C}_s = -\frac{C_o}{De} \tag{B13}$$

subject to:

$$\overline{C}_s\ (R_s, p) = \overline{C}_R(p) \tag{B14a}$$

$$\frac{d\overline{C}_s}{dr}(0,p) = 0 \tag{B14b}$$

The general solution to equation (B13), subject to (B14a) and (B14b) is:

$$\overline{C}_s = \left(\overline{C}_R - \frac{C_o}{P}\right)\frac{I_o(qr)}{I_o(qR_s)} + \frac{C_o}{P} \tag{B15}$$

where,

$$q = \left(\frac{P}{De}\right)^{1/2}$$

We then need:

$$\frac{d\overline{C}_s}{dr}\Big|_{r=Rs} = q\left(\overline{C}_R - \frac{C_0}{P}\right)\frac{I(qR_s)}{I_o(qR_s)} \tag{B16}$$

Now let us take the Laplace transform of equation (B1) to get:

$$pV_R\overline{C}_R = 2\pi R^2{}_s\theta De\frac{d\overline{C}s}{dx}\Big|_{x=0} - 2\pi R_s L_s\theta D_e\frac{\partial\overline{C}_s}{\partial r}\Big|_{r=Rs} \tag{B17}$$

and then substitute our equation (B10) and equation (B16) into equation (B17) to obtain:

$$pV_R\overline{C}_R = -2\pi R^2{}_s\theta De\left(\frac{P}{De}\right)^{1/2}\left[\overline{C}_R - \frac{C_o}{P}\right] - 2\pi R_s L_s\theta De\left(\frac{P}{De}\right)^{1/2}\left(\overline{C}_R - \frac{C_o}{P}\right)\frac{I(qR_s)}{I_o(qR_s)}, \tag{B18}$$

Rearranging equation (B18) gives rise to equation (B19) defined below,

$$\overline{C}_R\left(pV_R + 2\pi R^2{}_s\theta D\left(\frac{P}{D}\right)^{1/2} + 2\pi R_s L_s\theta D\left(\frac{P}{D}\right)^{1/2}\frac{I(qR_s)}{I_o(qR_s)}\right) = \frac{C_o}{P}\left[2\pi R^2{}_S\theta\left(\frac{P}{D}\right)^{1/2} + 2\pi R_s L_s\theta D\left(\frac{P}{D}\right)^{1/2}\frac{I(qR_s)}{I(qR_s)}\right]$$

or

$$\overline{C}_R = \frac{C_o}{P}\left[\frac{2\pi R^2{}_s\theta De\left(\frac{P}{De}\right)^{1/2} + 2\pi R_s L_s\theta De\left(\frac{P}{De}\right)^{1/2}\frac{I(qR_s)}{I(qR_s)}}{pV_R + 2\pi R^2{}_s\theta De\left(\frac{P}{De}\right)^{1/2} + 2\pi R_s L_s\theta De\left(\frac{P}{De}\right)^{1/2}\frac{I(qR_s)}{I(qR_s)}}\right] \tag{B19}$$

Note, the reservoir concentration is $C_R(t) = L^{-1}\left[\overline{C}_R\right]$ where, $L^{-1}[\ ]$ is the inverse Laplace transform operator.

R	≡	reservoir	R_R	=	reservoir radius
s	≡	sample	C_R	=	concentration in the reservoir
V_R	≡	reservoir fluid volume	C_s	=	concentration in the sample
Vs	≡	sample volume	C_o	=	initial concentration
L_R	=	reservoir length	θ	=	porosity
L_s	=	sample length	De	=	effective diffusivity
s	=	sample radius			